

Polymer Chemistry

Accepted Manuscript



This is an *Accepted Manuscript*, which has been through the Royal Society of Chemistry peer review process and has been accepted for publication.

Accepted Manuscripts are published online shortly after acceptance, before technical editing, formatting and proof reading. Using this free service, authors can make their results available to the community, in citable form, before we publish the edited article. We will replace this *Accepted Manuscript* with the edited and formatted *Advance Article* as soon as it is available.

You can find more information about *Accepted Manuscripts* in the [Information for Authors](#).

Please note that technical editing may introduce minor changes to the text and/or graphics, which may alter content. The journal's standard [Terms & Conditions](#) and the [Ethical guidelines](#) still apply. In no event shall the Royal Society of Chemistry be held responsible for any errors or omissions in this *Accepted Manuscript* or any consequences arising from the use of any information it contains.

Cite this: DOI: 10.1039/c0xx00000x

www.rsc.org/xxxxxx

ARTICLE TYPE

Polyphenylenes and the related copolymer membranes for electrochemical device applications

X. Zhang^a, T. Higashihara^b, M. Ueda^{b*} and L. Wang^{a*}

Received (in XXX, XXX) XthXXXXXXXXXX 20XX, Accepted Xth XXXXXXXXXXXX 20XX

DOI: 10.1039/b000000x

Electrochemical devices employing ion-conducting polymer electrolyte membranes (PEMs) are promising power sources for automotive and energy storage applications. The development for the next generation of membrane separator materials with excellent performance has been the aim of intense research, as the alternatives for the state-of-the-art perfluorosulfonic acid (PFSA) ionomers.

Polyphenylene (PP), as a branch of aromatic PEMs, provides advantages due to the high C-C bond dissociation energy (BDE) of the phenyl-phenyl group, and has drawn much attention. This review gives an overview of polyphenylenes and their derivatives for use in cationic/anionic fuel cell (FC) and vanadium redox flow battery (VRFB) applications. In the first section, membrane categories and synthetic strategies are summarized and analyzed. Secondly, the *ex situ* characterizations of membranes are briefly compared and discussed, comprising ion conductivities, mechanical properties, swelling state, fuel permeabilities, *etc.* Meanwhile, nano-scale morphological studies are examined to obtain an insightful understanding into the fundamental behaviors. Thirdly, membranes for electrochemical device applications are investigated, together with durability evaluation, using US. DOE target as a standard. Collectively, this review aims to provide a better understanding of factors of PP-based PEMs. Their perspectives of future trends are also commented.

1 Introduction

The current supply and availability of energy have been increasing around the world. The rapid increasing in the world population with the expected quality of life would be unsustainable without dramatic improvements in the control and efficiency of energy production, storage, and use. The high quality of life has been derived from the exploitation of fossil fuels, and significant scientific and technological innovations. Since the long term influences of increasing CO₂ emissions on the earth is still unknown, it is obvious that clean and sustainable energy resources are highly required, being independent of the use of fossil fuels.^{1,2}

Actually, several alternative energy conversion systems have been investigated over the past decades, as represented by battery technology. Fuel cells and alkaline ion and redox flow batteries are promising systems among electrochemical devices.³⁻¹¹ These systems rely on the performance of ion conducting polymer membranes as separators. The devices function only when the applied membranes could efficiently separate the electrodes and mediate the electrochemical reactions at the anode and cathode by ion conduction. Taking the harsh operating conditions into consideration, the development of membranes with a high ion conductivity and high stability is demanded.¹²⁻¹⁹

Ion conducting membranes could be divided into two parts, acidic and alkaline membranes, that is, proton exchange

membranes (PEMs) and anion exchange membranes (AEMs), respectively. Among the state-of-the-art PEMs, sulfonated perfluoropolymers, (PFSA, *e.g.*, Dupont's Nafion[®], 3M, Aquivion[®] membranes) have been widely used for PEMs due to their high proton conductivity and high chemical stability. By chemical modifications or stabilizations, their new products (*e.g.*, NRE212, PFA, Aquivion[™], *etc.*) can even withstand the high temperature of 120 °C.^{20,21} However, notable drawbacks, such as a harsh producing process, high cost, and fluoro-release problem still more or less restrict their practical use. Hence, a number of non-fluorinated acid ionomers, especially the sulfonated aromatic hydrocarbon polymers, have been widely studied as alternative PEMs. The typical PEM materials include sulfonated poly(ether ketone)s (SPEKs),^{22,23} sulfonated poly(arylene ether sulfone)s (SPAESs),^{24,25} sulfonated polyimides (SPIs),²⁶ and sulfonated poly(phenylene ether)s (SPPes),^{27,28} which have been well developed during the past two decades.

Anionic materials have also received much attention for use in alkaline fuel cells relative to the cationic systems. Due to the enhancement of the electrode reaction kinetics at the cathode as well as the possibility of using inexpensive metals, extensive studies have been conducted in this field utilizing some classical polymer backbone structures — poly(styrene)s,²⁹⁻³¹ poly(phenylene oxide)s,^{32,33} poly(arylene ether sulfone/ketone)s,³⁴⁻³⁶ *etc.* Followed by the Menshutkin reaction with a tertiary amine, pentamethyl guanidine or *N*-methylimidazole, anionic conductive functional groups could be

precisely introduced into the membrane.

In general, polyphenylenes (PPs) provide advantages as polymer electrolyte membranes due to the absence of hetero atom linkages in their polymer backbones. Due to the high C-C bond dissociation energy (BDE) of the phenyl-phenyl group (478.6 ± 6.3 KJ/mol, 298K, see Table 1),³⁷ these chemical stable polymers have drawn much attention as candidates for ion conducting membranes.

Table 1 Typical bond dissociation energies (BDEs) in polyatomic molecules.

Bond	D_{298}^0 / KJ mol ⁻¹	Ref
C ₆ H ₅ -C ₆ H ₅	478.6 ± 6.3	37
C ₆ H ₅ -CH ₂ C ₆ H ₅	383.7 ± 8.4	37
C ₆ H ₅ -OC ₆ H ₅	326.8 ± 4.2	37
C ₆ H ₅ -C(O)CH ₃	407.6 ± 4.6	37
C ₆ H ₅ -SC ₆ H ₅	327.6 ± 10.5	37,38

From the viewpoint of chemistry, there are three types of linkages in the polymer main chains, *i.e.*, the *ortho*- (*o*-), *meta*- (*m*-) and *para*- (*p*-) positions. However, due to the reactivity and steric hindrance problems, it is rather difficult to obtain poly(*o*-phenylene)s with high molecular weight (*MW*s). In contrast, the *meta*- linkage makes polymer chains more flexible and the introduction of a long alkoxy side chain would effectively prevent the planar arrangement. This results in shortening the π -conjugation lengths along the backbones of the poly(*m*-phenylene)s³⁹ and providing an improved processability and film forming property.

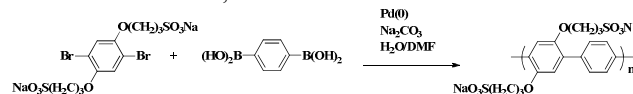
The most studied ionomers are poly(*p*-phenylene)s. The aromatic polymer main chains with a *para* linkage are exceptionally stable to hydrolysis and oxidation. However, based on coplanar molecular packing, these polymers generally exhibited a longer π -conjugation length in the solid state, resulting in a stiff rod-like feature. Moreover, their low solubility in most organic solvents produces difficulties in obtaining polymers with high *MW* during the polymerization, limiting the membrane forming process. In general, there are two strategies to overcome the aforementioned shortcomings. One is to directly introduce long side chains with sulfonated acid groups to the polymers. The other is to incorporate some flexible oligomers by chemical reaction (*e.g.*, block, grafting copolymerization, *etc.*).

In this review, an overview of polyphenylenes and their derivatives for use in cationic/anionic fuel cell (FC) and vanadium redox flow battery (VRFB) applications is presented. Because of the space limitation and the numerous of the relevant literature, references are restricted to some key papers, reviews, and our own work. For a broader view, the reader may refer to the huge number of papers in this field. The synthesis strategies, physicochemical properties, morphology, and cell performance are briefly reviewed and discussed.

2 Membrane category and synthesis

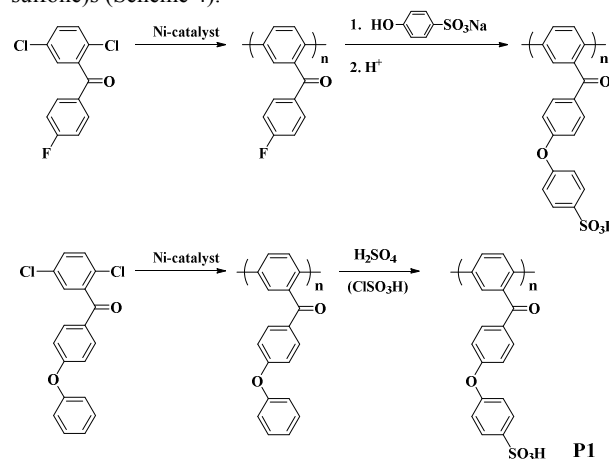
2.1 Sulfonated poly(*p*-phenylene)s

The typical synthetic method for sulfonated alkoxy PPs involves the Suzuki coupling reaction using dibromo- and diboronic acid-substituted monomers,⁴⁰ as shown in Scheme 1.

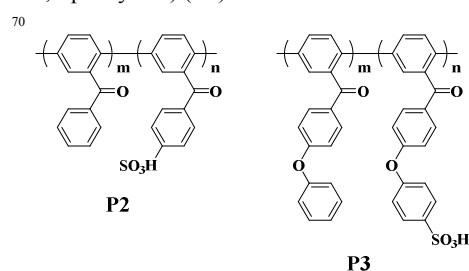


Scheme 1. Synthetic route of sulfonated alkoxy-substituted poly(*p*-phenylene) by Suzuki coupling reaction.⁴⁰

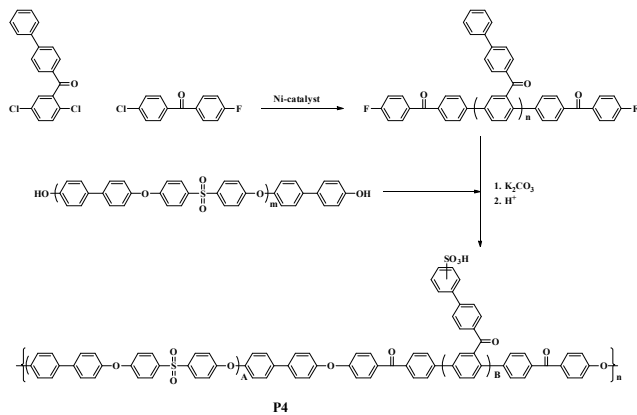
An alternative method was based on the coupling of substituted dichlorophenyl monomers using nickel catalysts with 2,5-dichlorobenzophenone (Scheme 2 and 3).⁴¹⁻⁴³ A sulfonated monomer was polymerized to afford sulfonated poly(*p*-phenylene)s (SPP) by nucleophilic substitution. However, chlorosulfonic acid or fuming sulfuric acid was typically employed as the sulfonation agents. The resulting polymers exhibited good solubility in polar aprotic solvents and could afford the self-standing membranes through the common casting processes.⁴³ Also, PPs could be incorporated into multiblock copolymers in conjunction with the segmented poly(arylene ether sulfone)s (Scheme 4).⁴⁴



Scheme 2. Synthetic route of sulfonated poly(4-phenoxybenzoyl-1,4-phenylene) (**P1**).^{41,43}

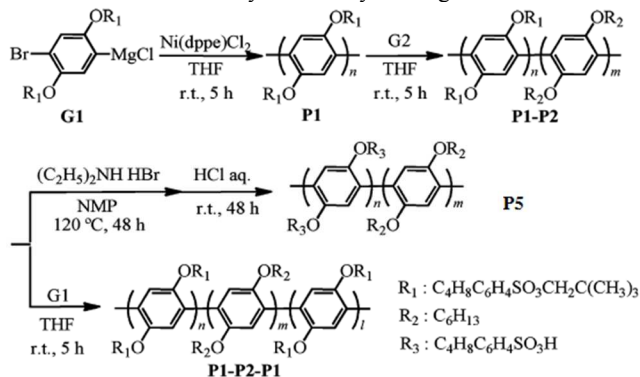


Scheme 3. Chemical structures of two types of sulfonated poly(*p*-phenylene) copolymers: sulfonated poly(*p*-benzoyl-phenylene) (sPBP, **P2**) and sulfonated poly(*p*-phenoxybenzoyl-1,4-phenylene) (sPPBP, **P3**).⁴²



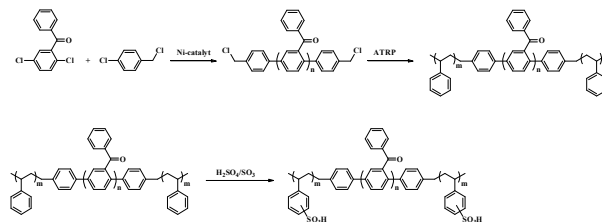
Scheme 4. Synthesis of sulfonated poly(*p*-phenylene)-based multiblock copolymers (**P4**).⁴⁴

A controlled polycondensation method, called catalyst transfer polycondensation, was applied to prepare PP block copolymers *via* a chain growth polymerization.⁴⁵⁻⁴⁷ Although it is widely considered that π -donor ability of thiophene ring is much stronger than that of phenylene ring, well defined diblock and triblock poly(*p*-phenylene)s were obtained with rather low dispersities (*D*).⁴⁵ As shown in Scheme 5, two electron-donating alkoxy side chains were initially introduced onto a Grignard-type monomer. Polymerization occurred in the presence of Ni(dppf)Cl₂ under mild condition with catalyst smoothly moving to the C-Br bond.



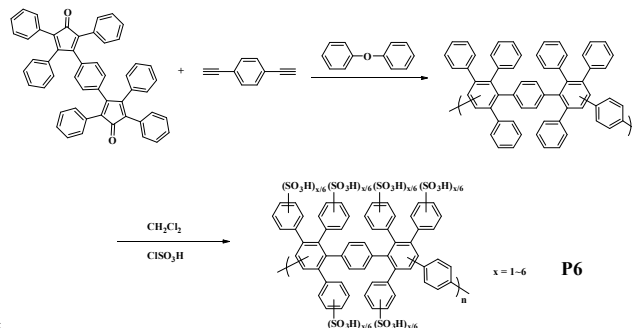
Scheme 5. Synthesis of SP1-P2 diblock (**P5**) and P1-P2-P1 triblock polymers.⁴⁵

Atom transfer radical polymerization (ATRP) was investigated to synthesize a tri-block (TB) copolymer, as shown in Scheme 6. The macroinitiator PP was first prepared by the nickel-catalyzed coupling reaction with benzyl chloride as the end-capped functional group, then styrene was added along with CuCl and various ligands.⁴⁸ As a result, TB copolymers were obtained with a low *D* value. Post-sulfonation successfully afforded a sulfonated TB copolymer. This TB copolymer showed a clear phase-separated morphology, which may be favorable for the formation of efficient proton conducting channels.



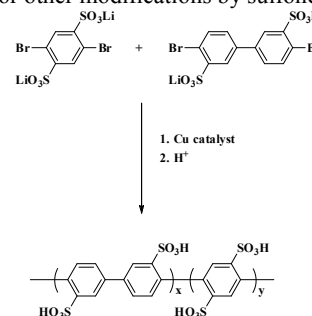
Scheme 6. Synthetic route of PP-based sulfonated triblock polymers.⁴⁸

Another method for the synthesis of poly(*p*-phenylene)s involves the Diels-Alder reaction.⁴⁹⁻⁵² Scheme 7 shows the synthesis and sulfonation processes of DA-sulfonated poly(*p*-phenylene) SPP ionomers (**P6**). Diels-Alder additions are generally regioselective, predominantly resulting in *para*-linkages of the polymer chain. However, regioselectivity may be lower in a sterically-crowded system, which would introduce a few flexible *meta*-linkages. Thus, these polymers may not be as strictly rod-like as the polymers prepared by nickel-catalytic aryl coupling. Their phenyl substituents provide a greater number of potential sites for sulfonation, which can also be achieved by further sulfonation.



Scheme 7. Synthetic route of DA-SPP (**P6**) from 1,4-bis(2,4,5-triphenylcyclopentadienone)benzene and di(ethynyl)benzene.⁴⁹

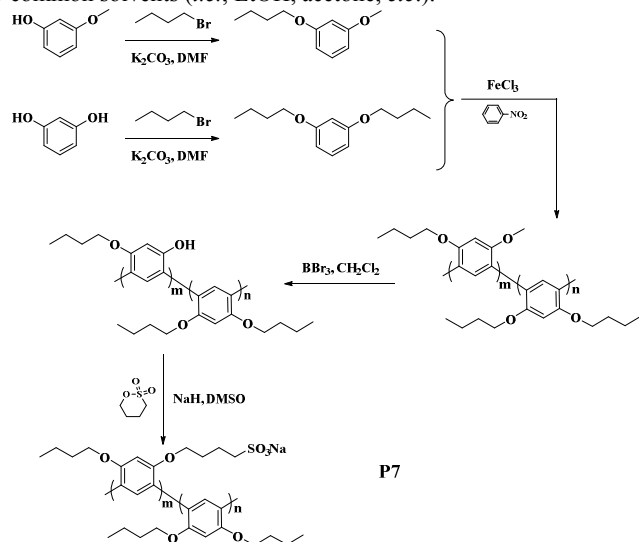
Another pathway to synthesize polyphenylenes is the Ullmann coupling of sulfonated dibromo biphenyl monomers. For this coupling reaction, it is useful to exchange the protons of the sulfonic acids for organic cations or metal ions, such as trimethyl benzylammonium or lithium ions.^{53,54} Scheme 8 shows the synthetic route of SPPs in the presence of a copper catalyst. After polymerization, these groups were then deprotected by an acid exchange process and some of the resulting sulfonic acid groups could be used for other modifications by sulfone formation.



Scheme 8. Synthetic route of SPP *via* the Ullmann reaction.⁵⁴

2.2 Sulfonated poly(*m*-phenylene)s

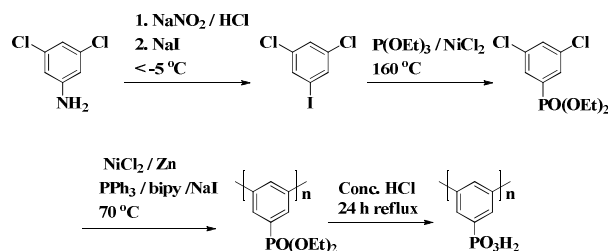
In principle, all dichloro- aromatic monomers could be coupled by nickel-catalyzed polymerization which has been used for the synthesis of poly(2-benzoyl-1,4-phenylene) as described above. However, there is a different and more straightforward approach to obtain poly(*m*-phenylene)s via oxidation polymerization in which the phenyl-phenyl linkage is at the *meta*-position. Typically, alkoxy groups or some ether linkages were initially introduced at the 1 and 3 positions onto the aromatic monomers so as to increase the electron density of the 4 and 6 positions, as shown in Scheme 9. The oxidation potentials were usually checked to evaluate the reactivity of the functional monomers. After polymerization, excessive oxidative reagents, such as FeCl₃ or VO(acac)₂, could be easily removed by rinsing with some common solvents (*i.e.*, EtOH, acetone, *etc.*).



Scheme 9. Synthetic routes for sulfonated poly(*m*-phenylene) copolymers (**P7**).⁵⁵

2.3 Phosphonated polyphenylenes

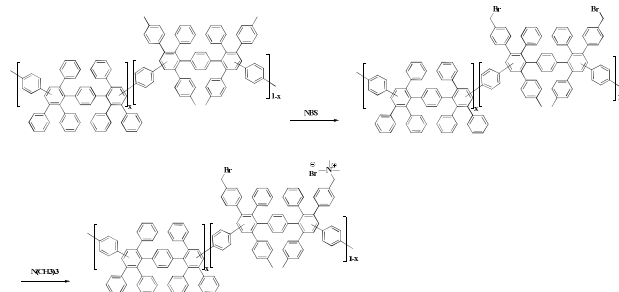
The phosphonated polyphenylenes, such as poly(1,3-phenylene-5-phosphonic acid), were reported by Rager *et al.*⁵⁷ A phosphonic acid ester group was primarily introduced into the aromatic monomer unit by the nickel-catalyzed Arbuzov reaction of an aryl bromide or -iodide with triethyl phosphite.⁵⁸ The aromatic rings were then linked together at the chlorinated positions by the nickel-catalyzed reductive coupling in the presence of metallic zinc.⁵⁹ The PPs with phosphonic acid groups were obtained by a final hydrolysis using concentrated HCl, as shown in Scheme 10.



Scheme 10. Synthesis of poly(*m*-phenylene phosphonic acid).⁵⁷

2.4 Anionic polyphenylenes

Similar to the DA-SPPs, the DA-PPs were utilized as anionic exchange membranes by the Sandia National Lab.^{60,61} As illustrated in Scheme 11, DA-quaternary ammonium PPs (DAQAPPs) were obtained by bromination of the benzylic methyl groups of the polymers, followed by the Menshutkin reaction with a tertiary amine or *N*-methylimidazole.⁶¹

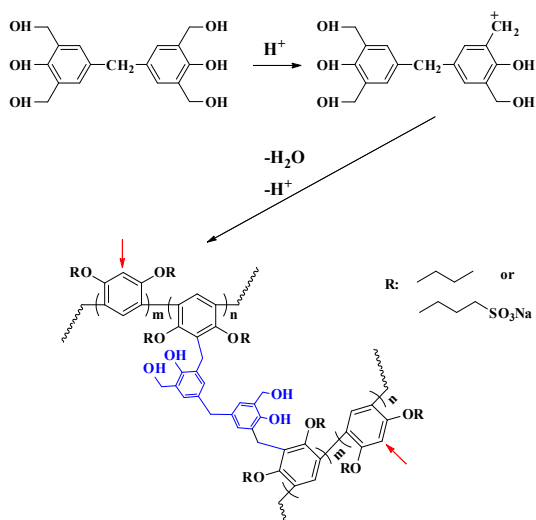
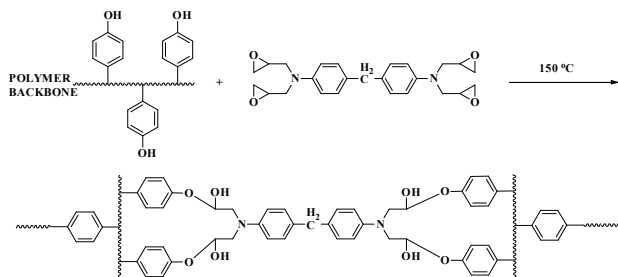


Scheme 11. Synthesis of DAQAPPs.⁶⁰

2.5 Cross-linking methods

In most cases, PP membranes were prepared by a solution casting method. A polymer was first dissolved in the proper medium to form a concentrated solution. To modify the properties of the membranes, some cross-linking reagents were simultaneously added to the polymer solution, if necessary. The solutions were cast and the excessive solvent was further evaporated at medium or high temperature. Finally, the as-prepared membranes were detached, washed with water, and followed by ion exchange processes for practical use.

The cross-linking reaction usually occurred in the presence of cross-linking reagents. Typically, the active hydroxyl groups were kept as the reaction initiation sites either in the polymer backbones or the bridges. Scheme 12 shows the mechanism of the cross-linking reaction by adding a multi-functional cross-linker, 4,4'-methylene-bis[2,6-bis(hydroxyethyl)phenol] (MBHP). The reaction occurred at the *ortho*- position of the alkoxy or ether linkage by the attack of a benzylic cation in the presence of acid.⁵⁵ Another method is to make a polymeric network by mixing the polymer and the epoxy-based agent during the membrane curing process,⁶² as shown in Scheme 13. However, the most widely applied pathway is still the intermolecular reaction between sulfonic acid and the phenyl groups, resulting in the sulfone bond forming. Normally, this approach takes place at a high temperature or in the presence of dehydration agents, *e.g.*, polyphosphoric acid (PPA) or P₂O₅.⁶³⁻⁶⁷

Scheme 12. Mechanism of cross-linking reaction with MBHP.⁵⁵Scheme 13. Cross-linking reaction in the presence of an epoxy-based crosslinker.⁶²

3 Membrane *ex situ* characteristics

3.1 Physico-chemical properties

Since SPPs have been recently developed, systematic data for their electrochemical and physical properties are rather limited. The first report was published by Rikukawa's group, in which two typical polymers of sulfonated poly(*p*-phenoxybenzoyl-1,4-phenylene, SPPBP) and sulfonated poly(ether ether ketone) (SPEEK) were investigated for comparison.^{43,68} Fig. 1 shows the conductivity data of these two types of membranes. At a similar degree of sulfonation (DS), SPPBP showed a better thermal stability, greater water uptake and proton conductivity under varied relative humidity (RH) conditions than the former.

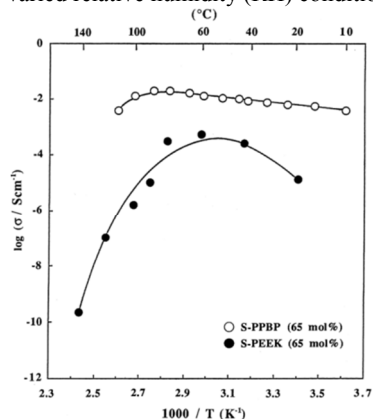


Fig. 1. Proton conductivities of S-PEEK and S-PPBP with 65 mol% sulfonation level under 100% relative humidity as a function of temperature.⁴³ Reprinted with permission from ref. 43. Copyright 1998 Elsevier.

A comparison between the **P2** and **P3** was made by Coutanceau's group.^{42,69} Both **P2** and **P3** are thermally stable up to at least 215 °C. The water uptake of the **P3** was found to be greater than that of the **P2**, *i.e.*, 65 and 43 mol%, respectively. Their permeability to methanol was found to be 10 times lower than that of Nafion 117 membrane. SPBP with alkyl side chains were then reported by Ohira *et al.*, as shown in Scheme 14.⁷⁰ The gas permeability of the **P8** under a wet condition was significantly affected by the length of the side chains, whereas the proton conductivity and water uptake were not, as shown in Fig. 2.

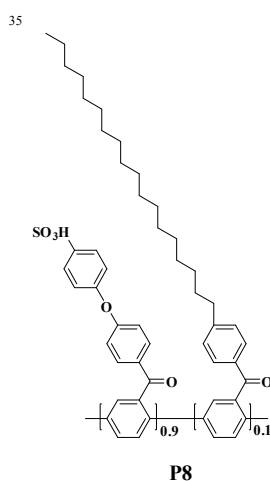
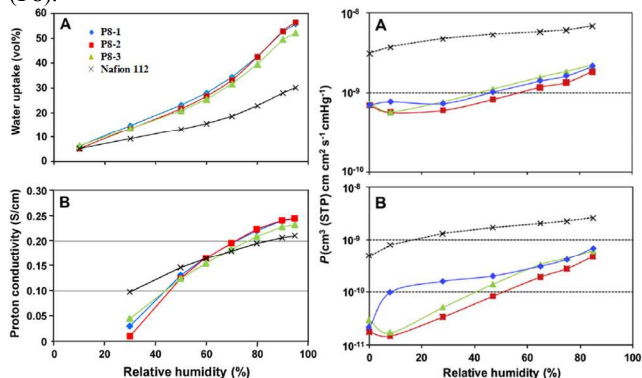
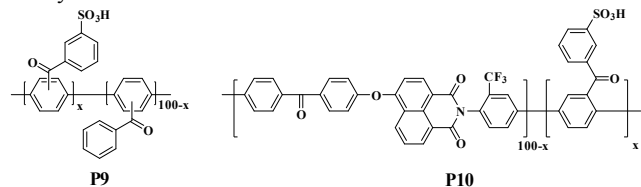
Scheme 14. Chemical structure of SPBP with alkyl side chains (**P8**).⁷⁰

Fig. 2. Relative humidity dependence of water uptake (left A), proton conductivity (left B) and gas permeability (H_2 , right A; O_2 , right B) of **P8-x** membranes at 80 °C (the IECs for **P8-1**, **P8-2** and **P8-3** are 2.53, 2.65 and 2.50 mequiv g^{-1} by back titration, respectively).⁷⁰ Reprinted with permission from ref. 70. Copyright 2010 Elsevier.

The properties of the SPP derivatives have been reported by many research groups. Zhang *et al.* directly introduced a sulfonic acid group onto the 2,5-dichlorobenzophenone monomer to get sodium 3-(2,5-dichlorobenzoyl)benzenesulfonate (DCBS) and copolymerized it with the precursor or some functional dichloro-

imide monomers *via* nickel-catalyzed coupling.⁷¹⁻⁷³ Scheme 15 lists the chemical structures of their copolymers. Compared to the ionomers obtained by post-sulfonation, these SPP derivatives could be prepared by a one-pot method, and the target *IEC* value could also be precisely controlled by adjusting the molar ratios of the monomers. The proton conductivity was also 2-3 times greater for **P9-70** (refers to 70% DS) than that of Nafion 117 in the hydrate state.



Scheme 15. Chemical structures of SPP copolymers (**P9** and **P10**).⁷¹⁻⁷³

Researchers from the JSR Corp., Japan, extensively investigated the sulfonated 1,4-phenylene monomers for PP-based multiblock copolymers (JSR membrane, **P11**).⁷⁴ Since the JSR electrolyte polymer has been designed with a rigid structure with a high water resistance, it is expected to have a 20-50% higher conductivity than the fluorinated membrane of Nafion 112 based on the results (Fig. 3). Anyway, the exact chemical structure of their hydrophobic moiety was unpublished due to industrial concerns.

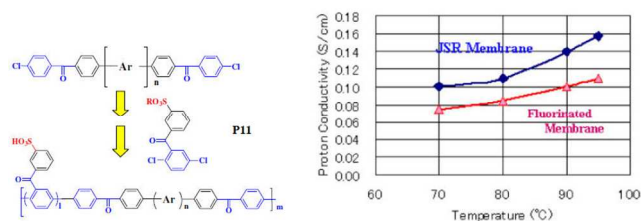
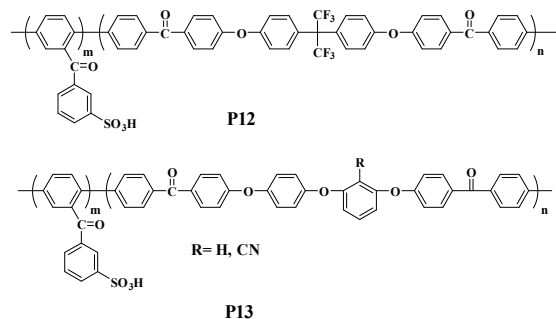


Fig. 3. Chemical structures and results of JSR membranes (**P11**).⁷⁴ Reprinted with permission from ref. 74. Copyright 2009 Nature Publishing Group.

Recently, Chen *et al.* prepared a series of SPP-*co*-PAEK copolymers by the coupling of two reactive functional monomers, 2,5-dichloro-3'-sulfobenzophenone and 2,2'-bis[4-(4-chlorobenzoyl)] phenoxy perfluoropropane, respectively (**P12** in Scheme 16).⁷⁵ A similar sulfonated poly(*p*-phenylene-*co*-arylene ether ketone) based on the benzonitrile group (**P13** Scheme 16) was also recently designed.⁷⁶ Strong interactions were found between the “-CN” and water molecules or other polar groups by an amorphous cell module simulation (Fig. 4), thus resulting in the decrease of the *WU* values and dimensional changes.



Scheme 16. Chemical structures of SPP-*co*-PAEK copolymers (**P12**⁷⁵ and **P13**⁷⁶).

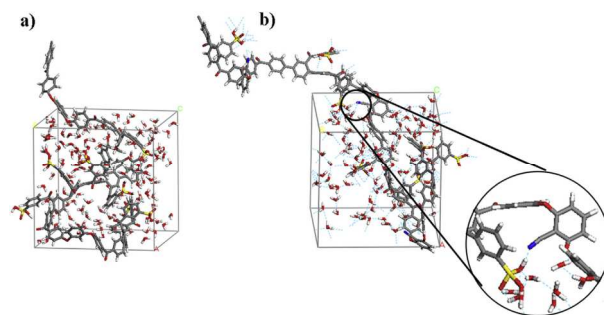
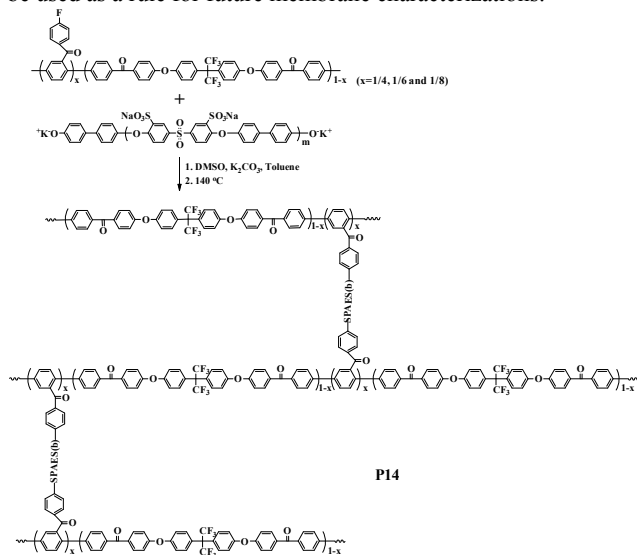


Fig. 4. Three-dimensional view of P13 in an amorphous periodic cell.⁷⁶ Reprinted with permission from ref. 76. Copyright 2014 Elsevier.

Novel sulfonated ionomers were developed utilizing poly(phenylene ether ketone) (PPEK) (segment 1) and a totally sulfonated poly(arylene ether sulfone) (segment 2) as backbones and graft pendants, respectively.⁷⁷ The synthetic route is shown in Scheme 17. The condensation reaction occurred between the functional fluorine group in segment 1 and the phenoxide-terminated groups in segment 2, and thus formed the graft cross-linked (GC, **P14**) architecture. The swelling state was anisotropic with some larger size changes in the thickness direction. It is worth noting that membranes showed a good proton conductive behavior with $\sigma_{\perp}/\sigma_{\parallel}$ (proton conductivity through-plane/in-plane) values in the range of 0.65-0.92. Considering the real proton conducting state in the fuel cell system, the evaluation of the anisotropic proton conduction ratio was quite essential and should be used as a rule for future membrane characterizations.



Scheme 17. Schematic diagram of the GC (**P14**) membranes.⁷²

A series of fully rigid-rod aromatic polysulfonic acids based on biphenyl backbones was prepared by Litt *et al.*^{63,64} A cross-linking reaction occurred in the presence of polyphosphoric acid (PPA) to form a network structure with a sulfone linkage (Fig. 5). The cross-linking degree was controlled by varying the reaction time and temperature. The *IEC* value of their membrane (**P15**)

was extremely high ($8.0 \text{ mequiv g}^{-1}$), which would be the highest value among the reported literature on sulfonated PEMs. However, all the films showed elastic moduli between 0.8 and 2.2 GPa with the break at 6 to 9% elongation at 22 to 30% RH. The proton conductivity was 4 to 5 times higher than that of Nafion over the entire RH range from 20 to 90%. Also, the through-plane proton conductivity was measured as a function of the RH. The data were nearly 0.1 S cm^{-1} under a $120 \text{ }^\circ\text{C}/30\% \text{ RH}$ condition, which reached the US. Department of Energy (US. DOE) 2015 target.

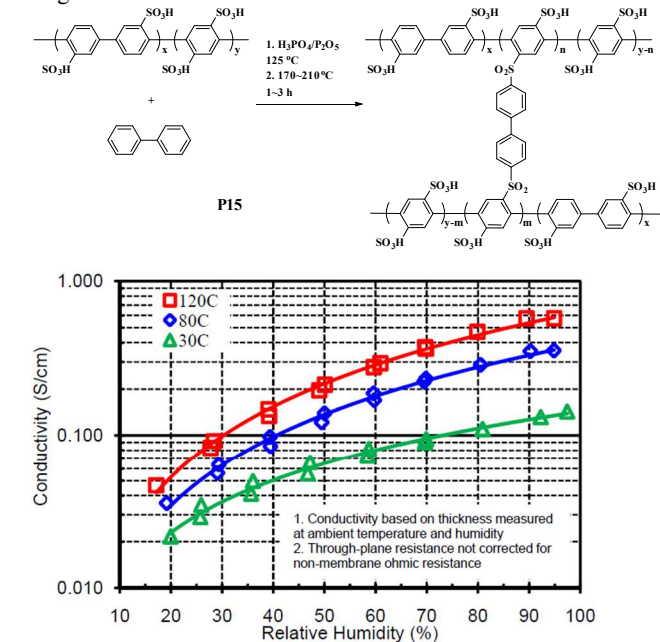


Fig. 5. Synthetic route of **P15** and the results of through-plane conductivity at varied T/RH% conditions.⁶⁴ Reprinted with permission from ref. 64. Copyright 2012 American Chemical Society.

3.2 Mechanical property

Mechanical stability is the key factor in determining the membrane strength and durability. Tensile-Stress (TS) is one of the conventional applied approaches to evaluate the membrane deformation resistance. Quite encouraging results were found on typical SPP-70 (**P9**), which exhibited a high storage modulus over 2.0 GPa and loss modulus over 0.2 GPa ranging from 100-450 $^\circ\text{C}$, respectively. The tensile strength and Young's modulus of the dry and hydrated membranes were more than 79 MPa and 20 MPa, and 1.7 GPa and 0.5 GPa, respectively, which indicated that these SPP membranes were strong and tough enough for fuel cell applications even with a high DS.⁷¹

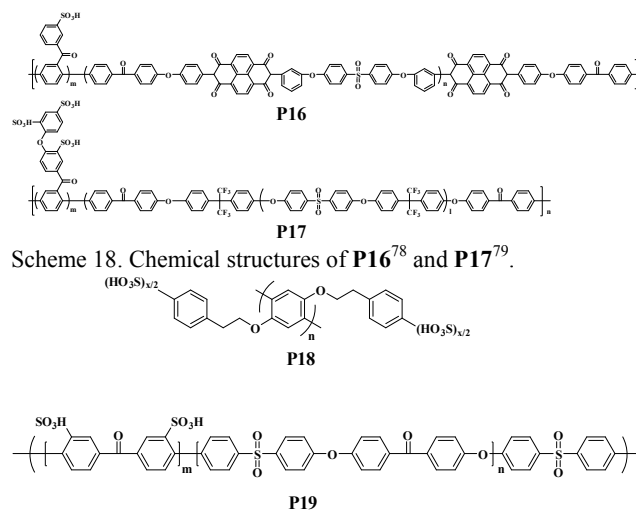
Nevertheless, it is considered that a polymer with backbones fully comprised of phenyl-phenyl bond tends to be brittle under high temperature condition, even if the *MW* is high enough. The membranes usually showed excellent tensile stress with a rather low elongation which would bring some difficulties in membrane electrode assembly (MEA) fabrication. Therefore, many researchers focused on SPP derivatives containing flexible linkages. By introducing the poly(arylene ether ketone) moiety, JSR membrane (**P11**) shows an elastic modulus of 1.8 GPa, a

tensile stress at yield of 83 MPa, a tensile stress at break of 130 MPa, and an elongation at break of 100%, exceeding the perfluorinated membrane by 10 times in elastic modulus and 2.6 times in tensile strength.⁷⁴ Not surprisingly, based on a PPEK polymer mainchain and SPAES side chain, the GC membranes also exhibited a reasonably high mechanical strength with Young's modulus, maximum stress and elongation at break values that ranged from 0.9 to 1.3 GPa, 31-49 MPa and 11-28%, respectively, under the $25 \text{ }^\circ\text{C}/50\% \text{ RH}$ condition.⁷⁷

Generally, tensile-stress measurement is useful to evaluate the membrane deformation ability especially during a hot-press procedure as well as the hydration-dehydration cycles in a fuel cell test. Therefore, the membrane with reinforced chemical structure tends to be an ideal material since it could effectively suppress the dimensional change.

Meanwhile, dynamic mechanical analysis (DMA) is also an insightful parameter which reflects the membrane creep resistance and glass transition temperature under varied conditions. Similarly, almost all the PPs exhibited E' (storage modulus) and E'' (loss modulus) of greater than 1.0 GPa and 1.0 MPa,^{55,71,73,74} respectively, indicating a good potential in high temperature and humidified operation.

Table 2 summarizes a comprehensive collection of characterization data on sulfonated polyphenylenes and their derivatives in which Nafion[®] is listed for comparison. The chemical structures of **P16-P19** are shown in Scheme 18 and 19.



Scheme 18. Chemical structures of **P16**⁷⁸ and **P17**⁷⁹.

Scheme 19. Chemical structures of **P18**⁸⁰ and **P19**⁸¹.

Cite this: DOI: 10.1039/c0xx00000x

www.rsc.org/xxxxxx

ARTICLE TYPE

Table 2 Physico-chemical properties of SPP and Nafion membranes.

Polymer	IEC mequiv g ⁻¹	Water uptake ^{a)} %	Swelling state ^{b)}		Proton conductivity ^{c)}		Fuel permeability			Young's modulus GPa	Reference
			Δ_l	Δ_t	50% RH	In water mS/cm	H ₂ 10 ⁻⁹ cm ³ (STD)	O ₂ cm cm ⁻² s ⁻¹ cm Hg ⁻¹	CH ₃ OH 10 ⁻⁷ cm ² s ⁻¹		
Nafion [®]	0.91	35~40	0.11~0.16		15~30	135~145	-	-	11~12	0.2~0.3	
P1	2.38	-	-	-	-	10	-	-	-	-	43
P2	0.70	43	-	-	-	-	-	-	1.4	-	69
P3	1.30	65	-	-	-	-	-	-	1.0	-	42
P4	1.20	50	-	-	-	36 ^{a)}	-	-	-	-	44
P5	2.42	-	-	-	ca. 130	>350(90%)	-	-	-	-	45
P6	1.80	75	-	-	-	87 ^{a)}	-	-	-	1.20	49
P7	2.93	67	0.16	0.16	31	251	-	-	-	-	55
P8	2.50	52(95%) ^{c)}	0.07	0.36	17	208(95%)	2.24 ^{e)}	0.627 ^{e)}	-	-	70
P9	2.78	54	-	-	-	174 ^{a)}	0.130 ^{d)}	0.010 ^{d)}	7.3	1.70	71
P10	2.00	72	0.09	0.21	-	321	-	-	6.2	1.26	73
P11	-	-	-	-	-	110(80%)	-	-	-	1.80	74
P12	1.98	55	0.12	0.13	7	164 ^{d)}	-	-	-	1.80	75
P13	1.90	43	0.10	0.13	-	ca. 100	-	-	2.3	0.70	76
P14	1.55	64	0.07	0.15	12	186 ^{d)}	-	-	-	1.33	77
P15	5.90	81	0.12	0.33	ca. 200	ca. 600(95%)	-	-	-	1.56	64
P16	1.92	73	0.11	0.31	36	203 ^{d)}	-	-	-	-	78
P17	1.21	25	0.05	0.09	14	146 ^{d)}	-	-	-	1.50	79
P18	2.49	222 ^{b)}	0.67	0.58	30	200(95%)	-	-	-	-	80
P19	2.08	30(90%) ^{c)}	-	-	30	ca. 300(95%)	0.140 ^{g)}	0.100 ^{g)}	-	-	81

a) At 30 °C in water; b) R. T. in water; c) At 80 °C; d) At 60 °C; the data in the parenthesis refer to the relative humidity condition; e) At 80 °C/85% RH; 10⁻⁹ cm³ (STP) cm cm⁻² s⁻¹ cm Hg⁻¹; f) About 80 °C, dry condition; g) At 80 °C/60% RH.

Cite this: DOI: 10.1039/c0xx00000x

www.rsc.org/xxxxxx

ARTICLE TYPE

3.3 Morphological studies

The morphological studies of SPP and derivatives have been extensively investigated. The structural anisotropy of the **P1** membranes was elucidated by Rikukawa *et al.* via polarized microscope measurements. **P1** with *IEC* values of 1.59-2.81 mequiv g⁻¹ showed typical colored nematic textures in a DMSO solution (Fig. 6), indicating a molecular organization of a rigid-rod lamellar structure, resulting in an anisotropic behavior during swelling.⁸²

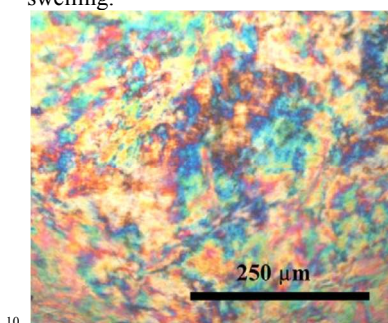


Fig. 6. Optical polarization micrograph of a 200 mg mL⁻¹ solution of **P1** (2.81 mequiv g⁻¹) in DMSO.⁸² Reprinted with permission from ref. 82. Copyright 2011 Elsevier.

The morphologies of the SPPs have also been characterized by high resolution transmission electron microscopy (TEM) and atomic force microscopy (AFM). These techniques provide direct visualization of the phase separation and the presence of ionic clusters in the membrane. For the polybenzophenone-based SPPs (**P9**), they displayed ionic domains with a size in the range of 10-30 nm, and the width increased with an increase in the *IEC* values, as shown in Fig. 7.⁷¹

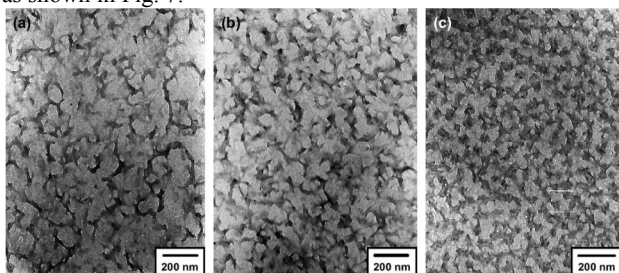


Fig. 7. TEM images of **P9-30** (a), **P9-50** (b) and **P9-70** (c), **P9-x**, where x refers to the DS.⁷¹ Reprinted with permission from ref. 71. Copyright 2006 Elsevier.

Researchers from the JSR Corp., comprehensively introduced the 4 strategies to control the film morphology.⁶⁹ (1) the mass ratio between the sulfonated and non-sulfonated moiety; (2) the chemical structure of the hydrophilic block; (3) the lengths of each block; and (4) the film casting conditions. As clearly seen in Fig. 8, the desired morphologies were obtained as designed

according to these parameters. The phase separation was clearly found for all of the membranes. The strip-like hydrophilic domains were well-connected to each other, and the aggregation became more obvious with increasing the block length ((a) vs (c); (b) vs (d)).

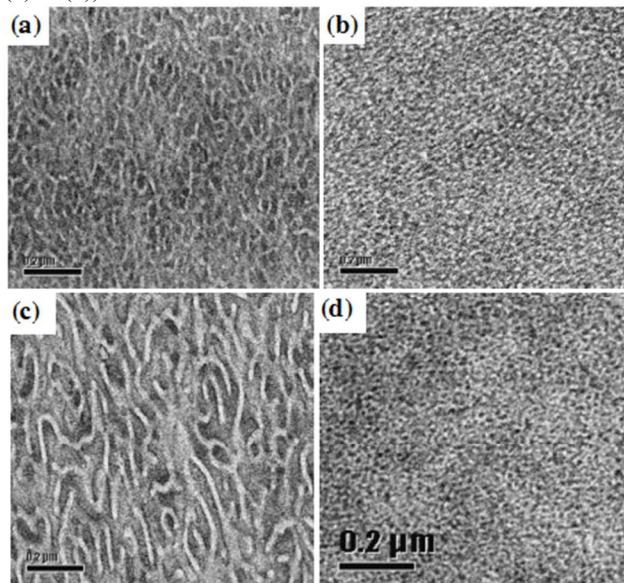


Fig. 8. Typical TEM images of **P11** membranes composed of different blocks, shorter blocks/low *IEC* (a), longer blocks/low *IEC* (c), shorter blocks/high *IEC* (b), longer blocks/high *IEC* (d).⁷⁴ Reprinted with permission from ref. 74. Copyright 2009 Nature Publishing Group.

It is interesting to study the morphology of a unique SPP derivative with densely located sulfonic acid groups.⁷⁹ Although the *IEC* value was as low as 1.21 mequiv g⁻¹, it still exhibited a well-defined microphase-separated structure with *ca.* 13-20 nm and 3-7 nm widths for the hydrophilic and hydrophobic domains, respectively (Fig. 9). This approximate isotropic phase separation would be one piece of direct evidence for the obtained high electrochemical performance, which will be discussed in the following section.

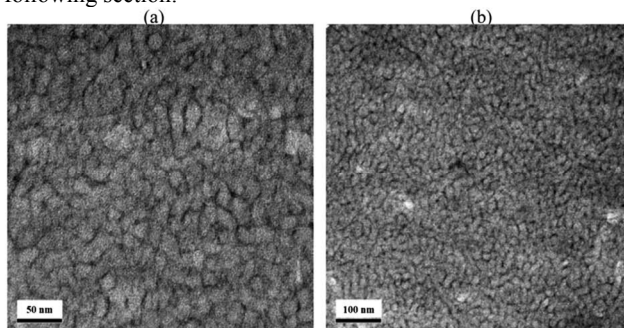
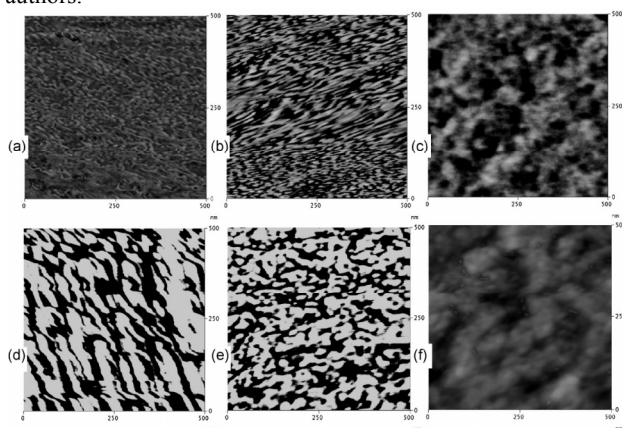


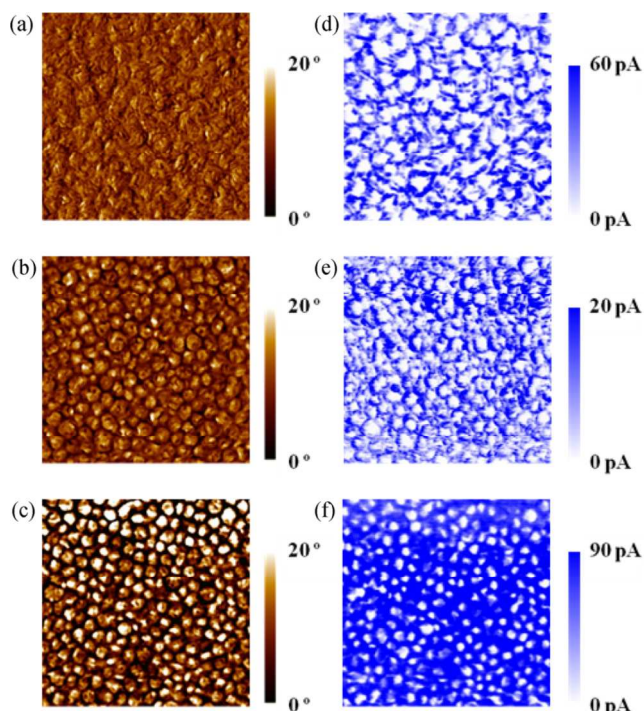
Fig. 9. TEM images of **P17** membranes stained with Cs⁺.

Acceleration voltage: (a) 50 kV; (b) 25 kV.⁷⁹ Reprinted with permission from ref. 79. Copyright 2013 Royal Society of Chemistry.

5 AFM has also been employed under various humidic conditions. Chen *et al.* used tapping-mode (TM) AFM to characterize the morphological positions of both ionic domains in their GC (**P14**) membranes,⁷⁷ as shown in Fig. 10. A well-defined nanoscale phase separation morphology was observed for all the
10 obtained GC membranes. Membrane **P14**(7/10) (*x/y* refers to the molar ratio of two dichloro- monomers and the length of the hydrophilic block moiety) with a low *IEC* (1.26 mequiv g⁻¹) exhibited a distinct phase separated morphology. The average width of the hydrophilic domains was about 25-35 nm, larger
15 than that of Nafion exposed to liquid water.⁸³ These discrepancies in the phase separations were closely related to the block length of the hydrophilic and hydrophobic units, as claimed by the authors.



20 Fig. 10. TM-AFM phase images: (a) **P14** (3/5); (b) **P14** (3/10); (c) **P14** (5/10); (d) **P14** (5/15); (e) **P14** (7/10); (f) **P14** (7/15).⁷⁷ Reprinted with permission from ref. 77. Copyright 2011 John Wiley & Sons, Inc.



25 Fig. 11. AFM phase (a–c) and current (d–f) images (1 × 1 μm) of polymer membranes: (a, d) **P5-1** (*IEC*=0.84 mequiv g⁻¹), (b, e) **P5-2** (*IEC*=1.77 mequiv g⁻¹), and (c, f) **P5-3** (*IEC*=2.20 mequiv g⁻¹) at 20 °C and 50% RH.⁴⁵ Reprinted with permission from ref. 45. Copyright 2012 American Chemical Society.

30

Fig. 11 shows the AFM phase and current images of **P5** membranes. Evidently, clear phase separations were observed for all the membranes. Both in the phase and current images, **P5** membranes showed sphere-like hydrophobic aggregates
35 surrounded by connected hydrophilic conducting domains. The aggregates became larger with increasing the *IEC* values, which were in good accordance with the proton transport behavior.⁴⁵

3.4 Chemical stability

For most cases, the chemical stability of the SPPs and derivatives
40 were estimated by accelerated *ex situ* tests, such as the oxidative test. As has been recognized that the formation and reactivity of free radical peroxide species are a major source of the degradation of the PEMs used in fuel cells, the oxidation test (so-called Fenton's test), using a H₂O₂ aqueous solution containing a
45 trace amount of Fe²⁺, has become a common accelerated test for membrane oxidative stability.⁸⁴⁻⁸⁶ In general, there were two methods: 1) by recording the elapsed time at which the membranes started to dissolve and completely dissolved in the solution; and 2) by the remaining weight of the residues after a
50 certain time period. Table 3 summarizes the reported chemical stabilities of the SPPs and derivatives based on Fenton's test. It should be mentioned that polyphenylenes with pendant sulfonic acid groups were more stable toward peroxide oxidation than the backbone-sulfonated PEMs. For instance, by comparison with a
55 well-developed multiblocked poly(arylene ether sulfone)s (*e.g.*, a typical membrane X15Y4 with an *IEC* of 2.01 mequiv g⁻¹, X, Y refer to the sulfonated "F-terminated" and "OH-terminated" oligomers, respectively; numbers refer to the chain length by calculation) which was completely dissolved in the aqueous

solution,⁸⁷ a polyphenylene with long sulfoalkyl side chains (*e.g.*, **P7**, $IEC = 2.93$ mequiv g^{-1}) still retained nearly 70% of the residual weight, indicating its excellent oxidation stability. Since it is widely considered that the electron-donating groups ($-O-$) in the *ortho*- and *para*- positions to the sulfonic acid group would stabilize the intermediate (so-called σ -complex, taken from the *ab-initio* calculation), and thus lead to a lower oxidative stability,⁸⁸⁻⁹⁰ the pendant sulfonated side chains would effectively avoid the radical-attack degradation.

10 Table 3 Oxidative results of some SPP derivatives.

Polymer ^{a)}	Fenton's reagent formulation	Temp./ °C	Degradation time ^{b)} /h	Remaining weight/%	Ref.
P9-50	30% H ₂ O ₂	25	57	-	71
P10	containing 30 ppm FeSO ₄	30	10	-	73
P7(5/5)	3% H ₂ O ₂	80 ^{c)}		93	55
P7(8/2)	containing 2 ppm FeSO ₄	80 ^{c)}		67	55

a) **P7(x/y)**, where x/y refers to the molar ratio of two functional monomers.

b) Elapsed times at which the membranes completely dissolve;

c) For 1 h.

15 Nevertheless, this method faces a limitation since there is sometimes a big discrepancy between the test results and the durability of the membranes during PEMFC operation.^{91,92} It is well accepted that perfluorosulfonic acid membranes afford an excellent chemical stability in Fenton's reagent, over hundreds to thousands of hours, however, they usually showed a much shorter life time in fuel cell applications. This rather poor correlation has been explained by the following considerations.⁹³ Generally, there is a complex combination of different degradation processes for PEMs in fuel cells which are strongly influenced by the membrane itself, fabrication, and operating conditions. The peroxide/radical degradation of Fenton's test cannot be the only measurement for the membrane lifetime prediction. On the one hand, the peroxide content in an accelerated Fenton's test is too high to compare with typical fuel cell operating conditions. On the other hand, a direct lifetime comparison among the different types of membranes is almost impossible when different fuel cell operating conditions are applied. The most significant key issue is that the gas permeation should be taken into consideration. Since the concentration of radicals in the MEAs partly depends on the gas permeability of the membranes, this parameter needs to be evaluated at the same time. Consequently, a sufficient understanding of the degradation on hydrocarbon membranes, especially on the SPPs and derivatives, still need to be further studied using different evaluation methods.

As for AEMs, hydroxide ion conductivities and stabilities are also the important physico-chemical properties, since they may directly determine the electro-performance in the fuel cell. The aforementioned DAQAPPs,⁶⁰ both for random and block copolymers, exhibited rather high " $-OH$ " conductivities ranging from 30-50 mS cm^{-1} , with the IEC value of 1.2-1.6 mequiv. g^{-1} , which were greater than some of the well-developed

poly(sulfone)-based AEMs.⁹⁴ This might be attributed to the irregularities of the polyphenylene backbone and bulky side groups which would effectively prevent the packing state in the polymer matrix. A comparison was done comprised of different cationic substituted groups,⁶¹ as shown in Fig. 12. Quaternary ammonium groups with only a benzylic methylene spacer to the polymer backbone showed the best durability with merely a 5% conductivity loss over two weeks in an alkali solution. This trend is also consistent with that in quaternized poly(2,6-dimethyl phenylene oxide)s; the shorter carbon chains result in the better stabilities.⁷

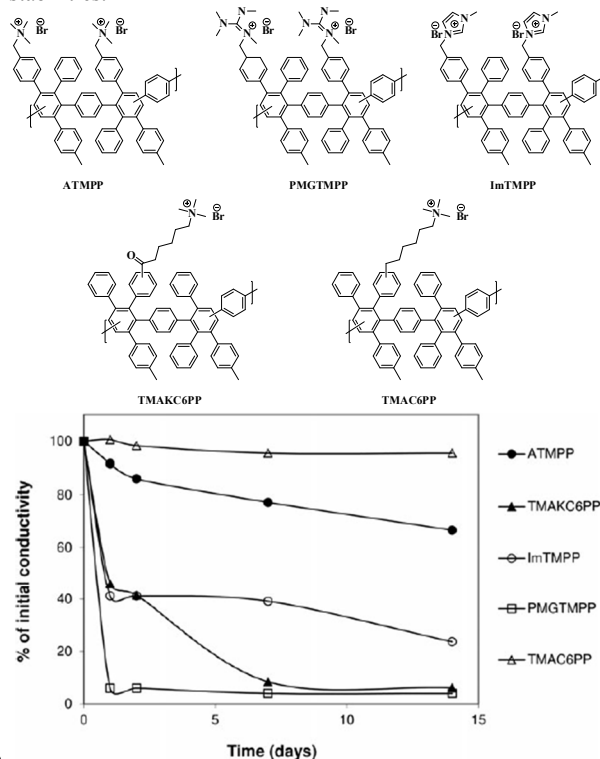


Fig. 12. Chemical structures and stabilities of DAQAPPs with different side chains.⁶¹ Reprinted with permission from ref. 61. Copyright 2012 John Wiley & Sons, Inc.

4 Electrochemical device applications

4.1 PEM H₂/O₂ Fuel Cells (PEMFC)

Cell performance is the most important *in situ* test for evaluating the electrochemical properties of PEMs in a fuel cell system. Although based on a high fuel crossover, PFSA ionomers have yet been used in most of cases even in the new generation fuel cell vehicles, otherwise the electrode performance are not very good.

However, the studies of the H₂/O₂ PEMFC performance based on a typical sulfonated polybenzophenone are also rather limited. The first report about the SPP-based H₂/O₂ fuel cell was published by Bae's group.⁴³ They characterized the I-V polarization curve of **P1** (sulfonation level 65%) at 80 °C using a commercial Pt/C electrode (E-TEK ELAT/Std. Electrode, Platinum loading of 0.4 mg cm^{-2}). The RHs of the cathode and anode were maintained at 100% and the total pressure of both sides was kept at 3 atm. The obtained cell voltage at a 0.8 A cm^{-2}

current density was 0.38 V with a maximum power output (P_{\max}) of only 300 mW cm⁻². The reason for this low performance might be attributed to the relatively low proton conductivity of their membranes.

Most of the presented PEMFC studies focused on the SPP derivatives. Okamoto *et al.* introduced the cell test for a series of imide-based block SPPs.⁷⁸ Membrane **P16** with a low IEC value of 1.51 mequiv g⁻¹ exhibited an acceptable PEMFC performance of (P_{\max} 0.76 mW cm⁻²) under the conditions of 90 °C, 80/80% RH (gas humidifier temperature of 85 °C), and 0.3 MPa. The high through-plane conductivity of **P16** (66 mS cm⁻¹ in water) contributed to this reasonably high performance.

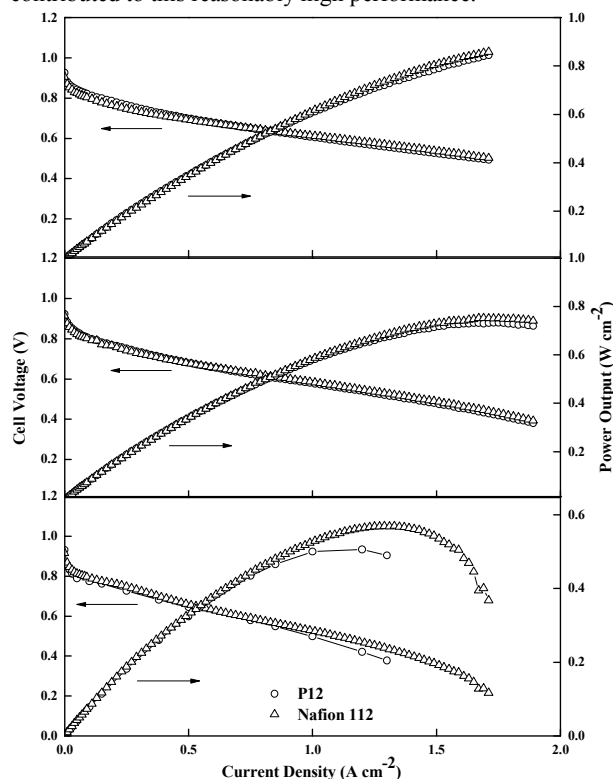


Fig. 13. Performance of PEMFCs with **P12** and Nafion 112 at 90 °C/0.2 MPa with supply of H₂/air and gas humidification of (a) 82/68% RH, (b) 48/48% and (c) 27/27% RH.⁷⁵ Reprinted with permission from ref. 75. Copyright 2012 Elsevier.

Recently, Chen *et al.* reported the PEMFC performance of SPP-co-PAEKs membranes, as shown in Fig. 13.⁷⁵ Under a mild operation condition (90 °C, 0.2 MPa, 82/68% RH), **P12** showed an excellent PEM fuel cell performance with the open circuit voltage (OCV) of 0.94 V, cell voltage at the current density of 1.0 A cm⁻² ($V_{1.0}$) of 0.61 V, and P_{\max} of 0.85 W cm⁻². The rigid poly(*p*-phenylene) linkages might make the hydrophilic moiety stack more tightly, resulting in a continuous proton conductive pathway and reasonably high cell performance.

Several extensive studies were pursued by Okamoto' group.^{79,95,96} **P17** with a low IEC of 1.21 mequiv g⁻¹ showed a rather high cell performance at 90 °C, 0.2 MPa and 82/68%RH, *i.e.*, $V_{0.5}$ of 0.72 V and P_{\max} of > 0.95 W cm⁻². These results might be the highest level for an SPP and derivatives among the reported literature. Either a decrease in the gas pressure from 0.2 MPa to 0.1 MPa (ambient pressure) at 82/68% RH or a decrease

in the gas humidification from 82/68% RH to 30% RH at 0.2 MPa caused a small reduction in the PEMFC performance. Another comparable result was for **P14** (3/10) (Fig. 14),⁹⁶ it showed a $V_{0.5}$ of 0.75 V and P_{\max} of 0.93 W cm⁻² under the same operation conditions as mentioned above. It is worth noting that the $V_{0.3}$ reached as high as 0.8 V, which just satisfies the US. DOE target 2020 (0.8 V), whereas the P_{\max} still needs to be further improved (US. DOE, 1.0 W cm⁻²).⁹⁷ Fig. 15 shows the durability test for **P14** (5/10) at 90 °C, 0.2 MPa and 50% RH under the constant load current density of 0.5 A cm⁻², while monitoring the cell voltage and cell resistance. The cell voltage and OCV were held almost aptotic with only slight decreases (0.03-0.04 V) for 1000 h. Meanwhile, the polarization and power output curves changed with a slight reduction in the PEMFC performance that occurred by 640 h, but no further reduction after 1000 h. This fully hydrophobic polyphenylene structure as the polymer backbone would effectively enhance the stability.

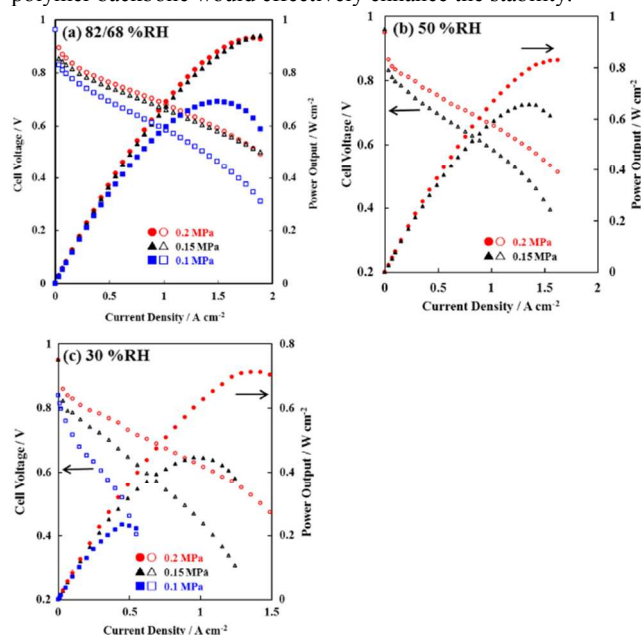


Fig. 14. Effect of feed gas pressure and humidification on PEMFC performances for **P14** (3/10) at 90 °C.⁹⁶ Reprinted with permission from ref. 96. Copyright 2014 Elsevier.

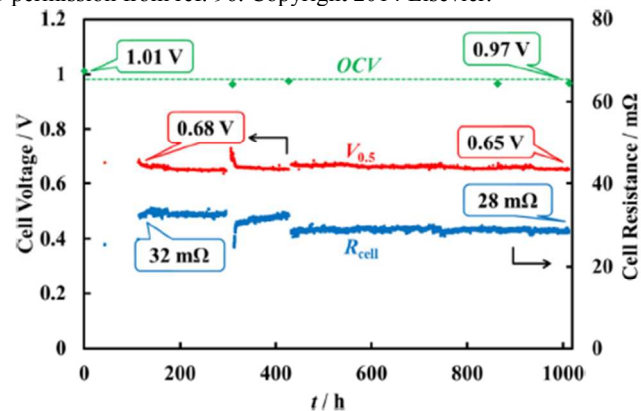


Fig. 15. Durability test of PEMFC with **P14**(5/10) at 90 °C, 0.15 MPa, 50% RH and 0.5 A cm⁻².⁹⁶ Reprinted with permission from ref. 96. Copyright 2014 Elsevier.

Miyatake *et al.* reported the cell performance of sulfonated polybenzophenone/poly(arylene ether) block copolymer membranes.⁸¹ Fig. 16 shows their PEMFC and durability results. A reasonably good performance was obtained at a high RH (80 and 100% RH, 80 °C, and ambient pressure), however, the performance became worse with the decreasing RH due to the rapid decrease in the proton conductivity. The cell voltage $V_{0.5}$ decreased from 0.69 V (100% RH) to 0.39 V (40% RH) for membrane **P19**. The durability was also acceptable with an *OCV* decrease from 1.07 V (initial) to 0.94 V (after 1100 h). However, it is not easy to directly compare the PEMFC performance for this type of membrane to those of Okamoto's due to the different operating conditions regarding the cell temperature and RHs.

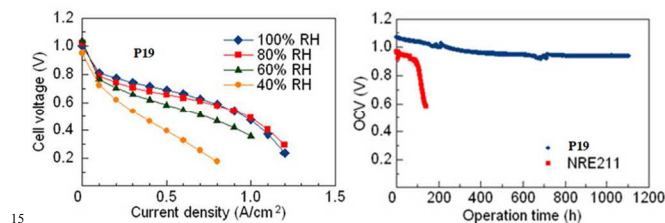
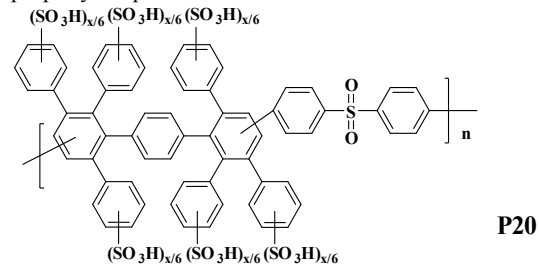


Fig. 16. PEMFC performance and durability of **P19**.⁸¹ Reprinted with permission from ref. 81. Copyright 2012 American Chemical Society.

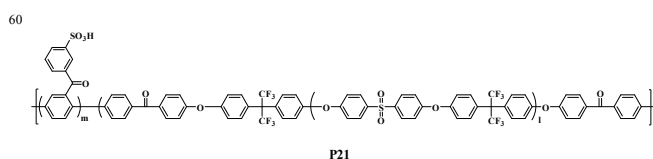
It is quite interesting to evaluate the PEMFC performance of high-*IEC* membranes.⁶⁴ The authors stated that the very low elongation at break caused problems during the MEA fabrication; the membranes easily broke during the hot-press procedure. However, a low *OCV* of 0.84 V was obtained by a non-hot-pressed membrane, indicating the high gas permeation. Also, the voltage curve significantly dropped below 1.0 A cm⁻², which was inferior to that of Nafion. High *IEC* values did not reflect the high electrochemical performance due to the extremely swelled state of the membranes. The *ex situ* characterization might cause significant errors if the membrane sheets were too small, since dimensional changes were somewhat imperceptible under these condition. However, the issue became more serious when the membranes underwent in the fuel cell test. Too high *IEC* values caused inneglectable large swellings, and seemed not to be properly adopted as PEM materials in the current situation.



Scheme 20. Chemical structures of **P20**.⁵²

The cell performance of the DA-SPPs were characterized by the Sandia National Laboratories.⁹⁸ Under an ideal condition (100% RH and pure O₂ as cathode gas), membrane **P6** with an *IEC* value of 2.3 mequiv g⁻¹ achieved 1.02 A cm⁻² at 0.65 V, which was 15% less than that of Nafion 212. Unfortunately, its performance rapidly decreased with a decreasing RH. The majority of the cell

losses at a low RH were due to the dramatic decreases in the proton conductivity. Recently, the electrochemical properties were characterized by Kim *et al.* based on a series of DA-sulfonated poly(phenylene sulfone)s (DA-SPPS, **P20**, see Scheme 20).⁵² Membrane with an *IEC* of 1.88 mequiv g⁻¹ exhibited a slightly higher cell performance than that of Nafion over the entire range of current densities, and P_{\max} was roughly 0.69 W cm⁻². DA-SPP and its derivatives showed a quite large RH dependence of PEMFC performance with acceptable data under high RH conditions. Considering their low electrochemical capacities derived from low proton conductivities at a low RH, a morphological study was essentially needed in order to simultaneously explore the polymer structure effect. An overview comparison data on PEMFC performance is summarized in Table 4 (The chemical structure of **P21** is shown in Scheme 21).



Scheme 21. Chemical structures of **P21**.⁹⁵

Table 4 PEMFC performance data of reported SPP membranes.

Conditions ^{a)}	Membrane	<i>OCV</i> / V	$V_{0.5}$ / V	P_{\max} W cm ⁻²	$\sigma_{\perp,FC}^{b)}$ mS cm ⁻¹	Ref
0.2/82 ^{c)}	P14 (3/10)	1.00	0.75	0.93	95	96
	P14 (5/10)	1.00	0.75	0.94	98	96
	P17	0.95	0.72	>0.95	74	79
	P21	0.95	0.72	>0.92	91	95
	P12	0.95	0.69	0.85	54	75
	P16	-	-	0.75 ^{d)}	-	78
0.1/82 ^{c)}	Nafion 112	0.95	0.71	>0.90	93	96
	P14 (3/10)	0.96	0.69	0.69	73	96
	P17	0.94	0.63	0.70	54	79
	P21	0.95	0.65	0.68	68	95
	P19 ^{e)}	1.00	0.69	-	-	81
0.1/50 ^{c)}	P6 ^{e)}	-	ca. 0.63	-	-	98
	Nafion 112	0.95	0.71	>0.90	93	96
	P17	0.93	0.60	0.46	36	79
	P21	0.95	0.59	0.42	39	95
0.1/30 ^{c)}	Nafion 112	0.95	0.60	0.39	36	96
	P14 (3/10)	0.94	0.46	0.23	(15)	96
	P19	-	0.39 ^{d)}	-	-	81

a) PEMFC operation conditions: x/y refers to gas pressure (MPa) and RH;

b) Recorded at 1.0 A cm⁻², the data in parentheses were measured at 0.5 A cm⁻²;

c) 82/62% RH;

d) At 0.3 MPa;

e) At 80 °C, 100% RH;

f) At 80 °C, 40% RH;

The fuel cell performance of DAQAPP anionic membranes was recorded with a high catalyst loading of 3 mg cm^{-2} at 60°C using H_2 and O_2 as fuels.⁹⁹ A high amount of the Pt catalyst was used to minimize the catalyst loss during the operation. A good performance was obtained with a P_{max} of 205 mW cm^{-2} at a current density of 0.4 A cm^{-2} (Fig. 17). However, a difference was found in these polymers with different *MW*s; the membrane with the lower *MW* exhibited a much higher cell resistance which resulted in the much poorer electrochemical performance. The mechanical strength was maintained without any abrupt drop during the short-term test, however, the increase in cell resistance (300%) and current density loss (*ca.* 70%) indicated a degradation of cation.

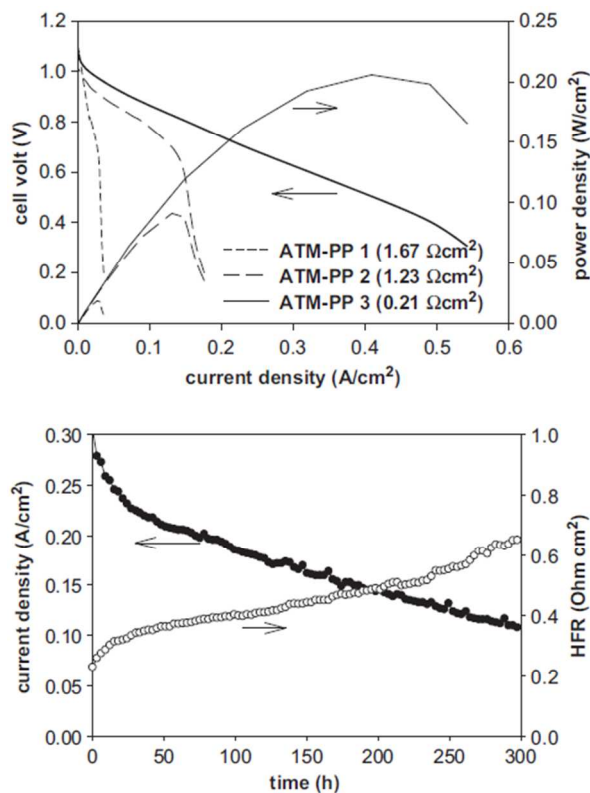
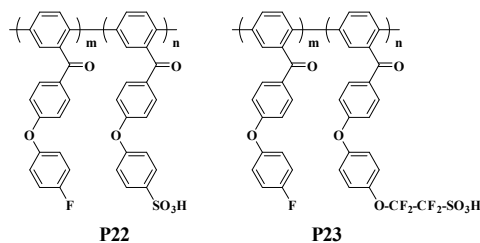


Fig. 17. H_2/O_2 fuel cell polarization curve at 60°C (upper); durability tests for DAQAPP (ATM-PP 3) membrane (bottom) (the *IECs* for ATM-PP 1, ATM-PP 2 and ATM-PP 3 are 1.3, 1.2 and 1.2 mequiv g^{-1} , respectively).⁹⁹ Reprinted with permission from ref. 99. Copyright 2012 Elsevier.

According to the mechanism of a fuel cell, it is desired to use a high-*IEC* membrane, since sufficient functional groups could facilitate ion conduction as well as the reduced cell resistance. However, these would consequentially raise the problem of excessive swellings, resulting in the detachment of catalyst layers. Meanwhile, the degradation always proceeds, especially when ion-rich polymers with electron-donating groups are used, as aforementioned. Therefore, the medium-*IEC* membranes comprising of a highly localized hydrophilic moiety and an indurative hydrophobic moiety would be the promising next generation electrolyte materials under the real operating condition.

4.2 Direct Methanol Fuel Cells (DMFCs)

The DMFC performance of SPP-based membranes was reported by Coutanceau's group in which three typical polybenzophenone-typed SPPs were compared.⁴² The membrane **P23** (Scheme 22), with a 5 times higher coefficient for methanol diffusion, still exhibited a better performance than the other two membranes (**P3** in Scheme 3 and **P22** in Scheme 22); the P_{max} reached 22 mW cm^{-2} at 0.11 mA cm^{-2} , whereas 10 and 15 mW cm^{-2} were obtained for the latter two. However, the data seemed to be rather inferior to some other reported sulfonated ionomers.¹⁰⁰⁻¹⁰³ This might be ascribed to the very low conductivity of the as-prepared membrane. Only 8.5 mS cm^{-1} was recorded at 20°C in the hydrate state, which was too low to obtain the ideal electrochemical performance.



Scheme 22. Chemical structures of **P22**, and **P23**.⁴²

Membrane electrode assemblies based on **P6** ionomers were also tested using 1 M and 3 M of liquid methanol as the fuels.⁹⁸ As shown in Fig. 18, no obvious difference was found for the power output in the high voltage and low current density region ($>0.4 \text{ V}$, $<0.1 \text{ A cm}^{-2}$, 1 M MeOH) for all the membranes, however, the conductivity effect became apparent at the higher current densities, indicating the non-ignorable current times resistance losses (*iR* losses). The DMFC performance decreased with the increasing methanol concentration to 3 M, which might be attributed to the higher fuel poisoning effect at the anode. Therefore, membranes with better methanol blocking capacities exhibited higher performances despite of the *IEC* values. By calculating the membrane fuel crossover, the reduction in methanol permeability on the order of 75% was required to mitigate the poisoning effect in the DMFC, as concluded by the authors.

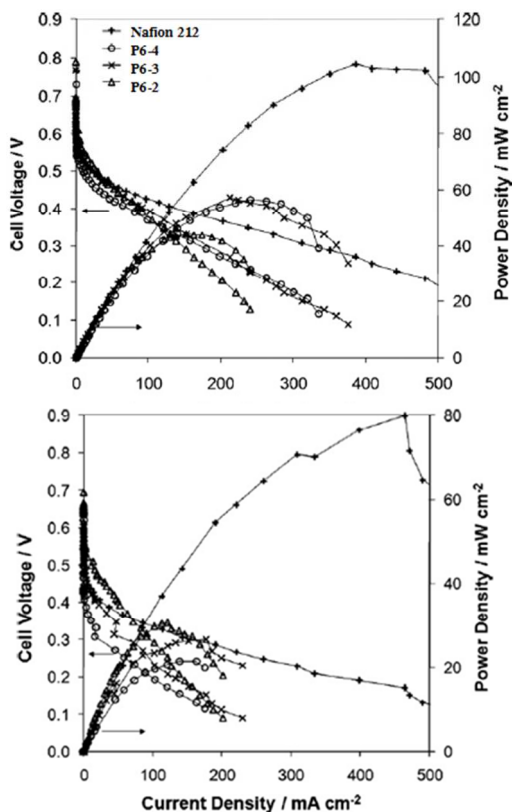


Fig. 18. DMFC performance of **P6-x** and Nafion (80 °C, 200 sccm of air fed to the cathode at 15 psig backpressure; 1.0 mL min⁻¹ methanol fed to anode at 0 psig backpressure: 1 M upper, 3 M bottom.) (the *IECs* for **P6-2**, **P6-3** and **P6-4** are 1.2, 1.7 and 2.3 mequiv g⁻¹, respectively).⁹⁸ Reprinted with permission from ref. 98. Copyright 2010 Elsevier.

An acceptable DMFC performance at room temperature was obtained by Zhang's group on **P13** copolymers,⁷⁶ as shown in Fig. 19. With a supply of 4 M methanol to the anode and air to the cathode, the **P13** (*IEC* = 1.86 mequiv. g⁻¹) membrane showed a P_{\max} of 24.5 mW cm⁻², which was comparable to that of Nafion 117 (24.3 mW cm⁻²) under the same operating conditions. The performance of **P13** membranes could be attributed to their high selective factor.

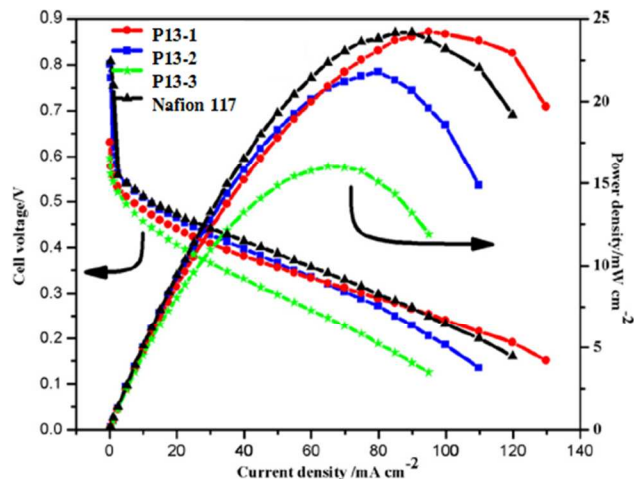


Fig. 19. Performance of DMFCs with Nafion 117 and **P13-x** copolymers membranes at 25°C under air-breathing mode with supply with 4 M methanol solution (the *IECs* for **P13-1**, **P13-2** and **P13-3** are 1.90, 2.12 and 2.17 mequiv g⁻¹, respectively).⁷⁶ Reprinted with permission from ref. 76. Copyright 2014 Elsevier.

On the one hand, the SPPs displayed a comparable low methanol permeation to some well-developed sulfonated ionomers,^{100,101} *i.e.*, a magnitude of 10⁻⁷, due to their rigid polymer skeletons. On the other hand, not completely satisfied performance was obtained. This might be due to the relatively low through-plane proton conductivities of these aforementioned polymers. Further studies regarding the proton conducting model of the DMFC system are also essential to understand the mass transfer mechanism.

Quite recently, a further improved DMFC performance was obtained for AEM (see Fig. 11, TMAC6PP) in the presence of hydroxide ions in the fuels.¹⁰⁶ The highest P_{\max} of 53.8 mW cm⁻² was generated in 1 M KOH at 226 mA cm⁻², and the power output did not show much decrease with lowering the KOH concentration to 0.5 M (45.5 mW cm⁻²). However, the poor performance was found with a supply of high concentration alkali solution. On the one hand, a stoichiometric amount of "OH⁻" was needed for methanol oxidation; the ions could also flush out the carbonate formed in the electrode along with the reaction. But too high "OH⁻" concentration in the fuels would inevitably increase the electrolyte viscosity and K₂CO₃ precipitation, as a result of pore obstruction and a dramatic rise resistance. On the other hand, the gas diffusion layer (GDL) materials were particularly applied with a hydrophilic anode and hydrophobic cathode. It has been demonstrated that the anode hydrophilicity would effectively enhance the MeOH diffusion, while the cathode hydrophobicity would prevent the water flooding.^{107,108} Therefore, the choice of GDL should be another issue in the future DMFC application.

4.3 Vanadium Redox Flow Batteries (VRFB)

Due to the similar roles as the separator and ion carrier, PEMs, which were used in fuel cells, were typically investigated for VRFBs applications.¹⁰⁹⁻¹¹⁴ The Sandia National Laboratory evaluated the VRFB performance of their **P6** polymers.¹¹⁵ Although these seemed to be some limitations for these materials as fuel cell membranes, their VRFB properties were quite encouraging. Regardless of the *IEC* values, all samples showed good columbic efficiencies (*CE*) and energy efficiencies (*EE*) of greater than 92% and 88%, respectively. Regarding the durability, the sulfonation degree strongly affected the operating cycles. A higher *IEC* value resulted in a lower cycle number as well as a faster degradation rate, as shown in Fig. 20.

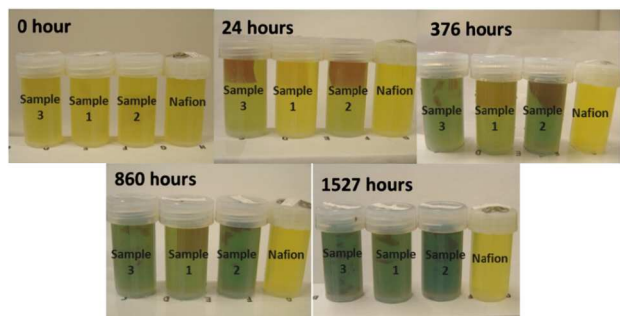


Fig. 20. Durability screening test of **P6** in V^{5+} solution.¹¹⁵ Reprinted with permission from ref. 115. Copyright 2012 Elsevier.

Analogously, DAQAPP membranes were also studied in a VRFB. The VO^{2+} permeation rate was proportional to the membrane *IEC* value, while the cell performance showed an opposite result. High *CE* and *EE* of 90-99% and 80-90% were obtained for all the DAQAPPs, respectively, which were comparable or higher than that of Nafion 212 (93 and 80%), as shown in Fig. 21. The durability of these ammonium functionalized membranes were found to be much better than those of the sulfonated ones (**P6**). Since the degradation largely depends on the *IECs*, the anionic membranes (low *IEC* values of 0.4-1.2 mequiv g^{-1}) exhibited no obvious oxidation and maintained their good shape over 2 weeks.¹¹⁶

Nowadays, the research on VRFB electrolytes shifts to not only the choice of materials themselves but also the morphological control, which is of crucial importance for the efficiency. Surface charging, compositing and pore size controlling (nanofiltration mode) were proved to have great contribution for increasing the ion selectivity¹¹⁷⁻¹²⁰. It is believed that the membranes with polyphenylene architectures would also have a bright future, coupled with these advanced technologies.

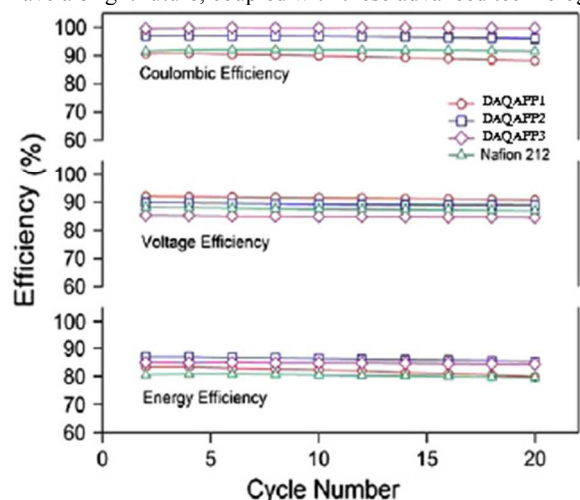


Fig. 21. Cycling efficiencies of DAQAPPs and Nafion 212. (the *IECs* for **DAQAPP1**, **DAQAPP2** and **DAQAPP3** are 1.20, 0.80 and 0.40 mequiv g^{-1} , respectively).¹¹⁶ Reprinted with permission from ref. 116. Copyright 2014 Elsevier.

5 Summary and Perspectives

As an important candidate for PEMs, polyphenylene and its

derivatives are promising for the commercialization of PEMFCs. Significant progress has been made in the development of SPPs with superior overall performances during the past decade. These membranes also exhibited many advantages under the harsh operation condition of acidic fuel cells due to their outstanding chemical stabilities. Recent achievements have been obtained by the polybenzophenone-based SPP derivatives. By chemical modification, the GC membranes (Chen's group) exhibited a distinct hydrophilic-hydrophobic microphase separation with a reasonable high proton conductivity and excellent PEMFC performance. The remarkable *OCV* and maximum power output were 0.94 V and 0.46 W cm^{-2} , respectively, even at 90 °C/30% RH, under ambient pressure.

Concerning the future prospective for the SPP related materials, their cost also needs to be taken into consideration. Although the cost of hydrocarbon monomers is quite low, the preparation of very complicated polymer structures or noble metal catalysts would inevitably increase the manufacturing costs. Meanwhile, post-sulfonation needs to be avoided due to use of a large excessive amount of halogenated solvents, long reaction time as well as some problems in acid-treatment.¹²¹ Sulfonated monomers are more preferred so that more approaches could be applied for molecular designs, however, a high purity is indeed required in order to obtain a polymer with a high *MW*. Durability would be another issue since more and more attention is being paid to practical fuel cell applications. The aforementioned GC ionomers and polybenzophenone-based main chain type SPP (Miyatake's group) have undergone over a thousand hours of fuel cell durability testing. JSR membranes even showed an endurance under rigorous conditions (110 °C, 50% RH) for over 1000 h. Nevertheless, the current progress is still far from the target by the US. DOE milestone 2015 (with a power degradation of less than 20%, and durability over 5000 h).

Studies of the PP-based AEMs are also interesting, since many SPP derivatives have already been used in the PEMFC system. The current state is quite encouraging with a power output comparable to some commercial AEMs. Future work should emphasize the stability research including the degradation mechanism.

The possibility for PP derivatives to be used as VRFB membranes is more promising due to the stable phenyl-phenyl bond which could survive under the highly oxidative operating conditions. Similar to the situation of PEMFCs, the durability is still a limiting factor for commercialization, although the *ex situ* performance is rather good. With scaling up to cell stacks, membrane swelling will become another important issue. Future detailed studies on the mass transfer mechanism and capacity fading during VRFB operation are highly demanded.

In conclusion, it is rather difficult to design or expect just a single type of PP derivative to meet all the requirements for electrochemical device applications. What is needed for future improvements rely on omnifarious efforts, including membranes, catalysts, a transport modeling study, technical assessments, *etc.*

Acknowledgment

This work is partly supported by Natural Science Foundation of Jiangsu Province (BK20140782), Jiangsu Key Laboratory of Chemical Pollution Control and Resources Reuse (NUST,

30920140122008), Industrial Technology Research Grant Program in 2011 (#11B02008c) from New Energy and Industrial Technology Development Organization (NEDO) of Japan.

Notes and references

⁵ ^a Jiangsu Key Laboratory of Chemical Pollution Control and Resources Reuse, School of Environmental and Biological Engineering, Nanjing University of Science and Technology, Nanjing 210094, Jiangsu Province, China; E-mail: wanglj@mail.njust.edu.cn (L. Wang)

^b Department of Polymer Science and Engineering, Faculty of Engineering, Yamagata University, 4-3-16 Jonan, Yonezawa City, Yamagata 992-8510, Japan; E-mail: ueda.m.ad@m.titech.ac.jp (M. Ueda)

- 1 B. Dunn, H. Kamath, J.-M. Tarascon, *Science*, 2011, **334**, 928.
- 2 International Energy Outlook. U.S. Energy Information Administration, 2013. <http://www.eia.gov/forecasts/ieo/>.
- 3 N. Li, M. D. Guiver, *Macromolecules*, 2014, **47**, 2175.
- 4 K. -D. Kreuer, *Chem. Mater.*, 2013, **26**, 361.
- 5 H. Zhang, P. K. Shen, *Chem. Rev.*, 2012, **112**, 2780.
- 6 Y. -L. Liu, *Polym. Chem.*, 2012, **3**, 1373.
- 7 N. Li, Y. Leng, M. A. Hickner, C. -Y. Wang, *J. Am. Chem. Soc.*, 2013, **135**, 10124.
- 8 N. Li, T. Yan, Z. Li, T. T. Albrecht, W. H. Binder, *Energy Environ. Sci.*, 2012, **5**, 7888.
- 9 J. Liu, J.-G. Zhang, Z. Yang, J. P. Lemmon, C. Imhoff, G. L. Graff, *et al.*, *Adv. Funct. Mater.*, 2013, **23**, 929.
- 10 P. Leung, X. Li, C. P. de Leo'n, L. Berlouis, C. T. J. Lowa and F. C. Walsh, *RSC Adv.*, 2012, **2**, 10125.
- 11 W. Wang, Q. Luo, B. Li, X. Wei, L. Li, and Z. Yang, *Adv. Funct. Mater.*, 2013, **23**, 970.
- 12 C. Vogel, J. M. -Haack, *Desalination*, 2014, **342**, 156.
- 13 H. Zhang, and P. K. Shen, *Chem. Soc. Rev.*, 2012, **41**, 2382.
- 14 J. Peron, Z. Shi and S. Holdcroft, *Energy Environ. Sci.*, 2011, **4**, 1575.
- 15 C. H. Park, C. H. Lee, M. D. Guiver, Y. M. Lee, *Prog. Polym. Sci.*, 2011, **36**, 1443.
- 16 Z. Mai, H. Zhang, X. Li, C. Bi, H. Dai, *J. Power Sources*, 2011, **196**, 482.
- 17 C. Ding, H. Zhang, X. Li, T. Liu, and F. Xing, *J. Phys. Chem. Lett.*, 2013, **4**, 1281.
- 18 M. J. Jung, J. Parrondo, C. G. Arges and V. Ramani, *J. Mater. Chem. A*, 2013, **1**, 10458.
- 19 S. Winardi, S. C. Raghu, M. O. Oo, Q. Yan, N. Wai, T. M. Lim, M. S. Kazacos, *J. Membr. Sci.*, 2014, **450**, 313.
- 20 S. Takamuku, P. Jannasch, *Adv. Energy Mater.*, 2012, **2**, 129.
- 21 M. Gebert, A. Ghielmi, L. Merlo, M. Corasaniti, V. Arcella, *ECS Trans.*, 2010, **26**, 279.
- 22 K. Matsumoto, T. Higashihara, M. Ueda, *Macromolecules*, 2008, **41**, 7560.
- 23 J. Pang, K. Shen, D. Ren, S. Feng, Z. Jiang, *J. Power Sources*, 2013, **226**, 179.
- 24 B. Lafitte, P. Jannasch, *Adv. Funct. Mater.*, 2007, **17**, 2823.
- 25 C. Wang, D. W. Shin, S. Y. Lee, N. R. Kang, Y. M. Lee, M. D. Guiver, *J. Membr. Sci.*, 2012, **405-406**, 68.
- 26 J. Yan, X. Huang, H. D. Moore, C. -Y. Wang, M. A. Hickner, *Int. J. Hydrogen Energy*, 2012, **37**, 6153.
- 27 T. Xu, D. Wu, L. Wu, *Prog. Polym. Sci.*, 2008, **33**, 894.
- 28 Z. Zhang, L. Wu, T. Xu, *J. Membr. Sci.*, 2011, **373**, 160.
- 29 Y. Luo, J. Guo, C. Wang, D. Chu, *J. Power Sources*, 2010, **195**, 3765.
- 30 J. R. Varcoe, R. C. T. Slade, E. L. H. Yee, S. D. Poynton, D. J. Driscoll, D. C. Apperley, *Chem. Mater.*, 2007, **19**, 2686.
- 31 L. Wang, and M. A. Hickner, *Polym. Chem.*, 2014, **5**, 2928.
- 32 N. Li, L. Wang and M. Hickner, *Chem. Commun.*, 2014, **50**, 4092.
- 33 Z. Zhang, L. Wu, T. Xu, *J. Membr. Sci.*, 2011, **373**, 160.
- 34 M. Tanaka, K. Fukasawa, E. Nishino, S. Yamaguchi, K. Yamada, H. Tanaka, B. Bae, K. Miyatake, and M. Watanabe, *J. Am. Chem. Soc.*, 2011, **133**, 10646.
- 35 F. Zhang, H. Zhang and C. Qu, *J. Mater. Chem.*, 2011, **21**, 12744.
- 36 D. Chen, and M. A. Hickner, *ACS Appl. Mater. Interfaces*, 2012, **4**, 5775.
- 37 Y. R. Luo, Comprehensive Handbook of Chemical Bond Energies, CRC Press, 2007.
- 38 R. L. David, CRC Handbook of Chemistry and Physics, 90th Edition. CRC Press, 2010.
- 39 T. Okada, N. Fujiwara, T. Ogata, O. Haba, M. Ueda, *J. Polym. Sci. A, Polym. Chem.*, 1997, **35**, 2259.
- 40 A. D. Child, J. R. Reynolds, *Macromolecules*, 1994, **27**, 1975.
- 41 H. Ghassemi, J. E. McGrath, *Polymer*, 2004, **45**, 5847.
- 42 C. Le. Ninivin, A. B. Longeau, D. Demattai, P. Palmas, J. Saillard, C. Coutanceau, C. Lamy, J. M. Leger, *J. Appl. Polym. Sci.*, 2006, **101**, 944.
- 43 T. Kobayashi, M. Rikukawa, K. Sanui, N. Ogata, *Solid State Ionics*, 1998, **106**, 219.
- 44 H. Ghassemi, G. Ndip, J. E. McGrath, *Polymer*, 2004, **45**, 5855.
- 45 K. Umezawa, T. Oshima, M. Y.-Fujita, Y. Takeoka, and M. Rikukawa, *ACS Macro Lett.*, 2012, **1**, 969.
- 46 T. Yokozawa, A. Yokoyama, *Chem. Rev.*, 2009, **109**, 5595.
- 47 S. R. Lee, J. W. G. Bloom, S. E. Wheeler and A. J. McNeil, *Dalton Trans.*, 2013, **42**, 4218.
- 48 E. C. Hagberg, B. Goodridge, O. Ugurlu, S. Chumbley, V. V. Sheares, *Macromolecules*, 2004, **37**, 3642.
- 49 C. H. Fujimoto, M. A. Hickner, C. K. Cornelius, D. A. Loy, *Macromolecules*, 2005, **38**, 5010.
- 50 R. J. Stanis, M. A. Yaklin, C. J. Cornelius, T. Takatera, A. Umemoto, A. Ambrosini, C. H. Fujimoto, *J. Power Sources*, 2010, **195**, 104.
- 51 *US. Pat.*, 8110636 B1, 2012.
- 52 Y. Lim, H. Lee, S. Lee, H. Jang, M. A. Hossain, Y. Cho, T. Kim, Y. Hong, W. Kim, *Electrochim. Acta.*, 2014, **119**, 16.
- 53 *US. Pat.*, 20050239994 A1, 2005.
- 54 K. Si, D. X. Dong, R. Wycisk, M. Litt, *J. Mater. Chem.*, 2012, **22**, 20907.
- 55 X. Zhang, L. Sheng, T. Higashihara, M. Ueda, *Polym. Chem.*, 2013, **4**, 1235.
- 56 V. Percec, S. Okita, J. H. Wang, *Macromolecules*, 1992, **25**, 64.
- 57 T. Rager, M. Schuster, H. Steininger, and K. -D. Kreuer, *Adv. Mater.*, 2007, **19**, 3317.
- 58 T. M. Balthazor, R. C. Grabiak, *J. Org. Chem.*, 1980, **45**, 5425.
- 59 D. Poppe, H. Frey, K.-D. Kreuer, A. Heinzl, R. Mülhaupt, *Macromolecules*, 2002, **35**, 7936.
- 60 M. R. Hibbs, C. H. Fujimoto, C. J. Cornelius, *Macromolecules*, 2009, **42**, 8316.
- 61 M. R. Hibbs, *J. Polym. Sci., Part B: Polym. Phys.*, 2012, **51**, 1736.
- 62 *US. Pat.*, 7816482B1, 2010.
- 63 K. Si, M. H. Litt, *ECS Trans.*, 2011, **41**, 1645.
- 64 K. Si, R. Wycisk, D. Dong, K. Cooper, M. Rodgers, P. Brooker, D. Slattery, M. Litt, *Macromolecules*, 2013, **46**, 422.
- 65 H. Hou, M. L. Di Vona, P. Knauth, *J. Membr. Sci.*, 2012, **423-424**, 113.
- 66 X. Zhang, Z. Hu, S. Zhang, S. Chen, S. Chen, J. Liu, L. Wang, *J. Appl. Polym. Sci.*, 2011, **121**, 1707.
- 67 J. Fang, F. Zhai, X. Guo, H. Xu and K. Okamoto, *J. Mater. Chem.*, 2007, **17**, 1102.
- 68 J. M. Bae, I. Honma, M. Murata, T. Yamamoto, M. Rikukawa, N. Ogata, *Solid State Ionics*, 2002, **147**, 189.
- 69 C. L. Ninivin, A. B. Longeau, D. Demattai, C. Coutanceau, C. Lamy and J. M. Leger, *J. Appl. Electrochem.*, 2004, **34**, 1159.
- 70 S. Seesukphronrarak, K. Ohira, K. Kiden, N. Takimoto, C. S. Kuroda, A. Ohira, *Polymer*, 2010, **51**, 623.
- 71 S. Wu, Z. Qiu, S. Zhang, X. Yang, F. Yang, Z. Li, *Polymer*, 2006, **47**, 6993.
- 72 Z. Qiu, S. Wu, Z. Li, S. Zhang, W. Xing, C. Liu, *Macromolecules*, 2006, **39**, 6425.
- 73 W. Li, Z. Cui, X. Zhou, S. Zhang, L. Dai, W. Xing, *J. Membr. Sci.*, 2008, **315**, 172.
- 74 K. Goto, I. Rozhanskii, Y. Yamakawa, T. Otsuki, Y. Naito, *Polym. J.*, 2009, **41**, 95.
- 75 X. Zhang, Z. Hu, Y. Pu, S. Chen, J. Ling, H. Bi, S. Chen, L. Wang, K. Okamoto, *J. Power Sources*, 2012, **216**, 261.
- 76 Q. He, J. Zheng, S. Zhang, *J. Power Sources*, 2014, **260**, 317.

- 77 X. Zhang, Z. Hu, L. Luo, S. Chen, J. Liu, S. Chen, L. Wang, *Macromol. Rapid Commun.*, 2011, **32**, 1108.
- 78 H. Bi, S. Chen, X. Chen, K. Chen, M. Higa, N. Endo, K. Okamoto, L. Wang, *Macromol. Rapid Commun.*, 2009, **30**, 1852.
- 79 S. Chen, R. Hara, K. Chen, X. Zhang, N. Endo, M. Higa, K. Okamoto and L. Wang, *J. Mater. Chem. A*, 2013, **1**, 8178.
- 80 K. Nakabayashi, K. Matsumoto, Y. Shibasaki, M. Ueda, *Polymer*, 2007, **48**, 5878.
- 81 T. Miyahara, T. Hayano, S. Matsuno, M. Watanabe, and K. Miyatake, *ACS Appl. Mat. Interfaces*, 2012, **4**, 2881.
- 82 I. Tonzuka, M. Yoshida, K. Kaneko, Y. Takeoka, M. Rikukawa, *Polymer*, 2011, **52**, 6020.
- 83 R. S. McLean, M. Doyle, B. B. Sauer, *Macromolecules*, 2000, **33**, 6541.
- 84 D. E. Curtin, R. D. Lousenberg, T. J. Henry, P. C. Tangeman, M. E. Tisack, *J. Power Sources*, 2004, **131**, 41.
- 85 T. Kinumoto, M. Inaba, Y. Nakayama, K. Ogata, R. Umebayashi, A. Tasaka, Y. Iriyama, T. Abe, Z. Ogumi, *J. Power Sources*, 2006, **158**, 1222.
- 86 H. Hou, M. L. D. Vona, P. Knauth, *ChemSusChem*, 2011, **4**, 1526.
- 87 B. Bae, T. Hoshi, K. Miyatake, and M. Watanabe, *Macromolecules*, 2011, **44**, 3884.
- 88 M. Schuster, K. D. Kreuer, H. T. Andersen, and J. Maier, *Macromolecules*, 2007, **40**, 598.
- 89 M. Schuster, C. C. Araujo, V. Atanasov, H. T. Andersen, and K. D. Kreuer, and J. Maier, *Macromolecules*, 2009, **42**, 3129.
- 90 J. O. Morley, and D. W. Roberts, *J. Org. Chem.*, 1997, **62**, 7358.
- 91 B. Bae, K. Miyatake, M. Uchida, H. Uchida, Y. Sakiyama, T. Okanishi, and M. Watanabe, *ACS Appl. Mat. Interfaces*, 2011, **3**, 2786.
- 92 D. P. Wilkinson and J. St-Pierre, *Handbook of Fuel Cells-Fundamentals, Technology and Application*. John Wiley & Sons, Ltd., 2010.
- 93 R. Borup, J. Meyers, B. Pivovar, Y. S. Kim, R. Mukundan, *et al.*, *Chem. Rev.*, 2007, **107**, 3904.
- 94 Z. Zhao, F. Gong, S. Zhang, S. Li, *J. Power Sources*, 2012, **218**, 368.
- 95 S. Chen, K. Chen, X. Zhang, R. Hara, N. Endo, M. Higa, K. Okamoto, L. Wang, *Polymer*, 2013, **54**, 236.
- 96 R. Hara, N. Endo, M. Higa, K. Okamoto, X. Zhang, H. Bi, S. Chen, Z. Hu, S. Chen, *J. Power Sources*, 2014, **247**, 932.
- 97 Department of Energy Hydrogen and Fuel Cells Program, Fuel Cell Technologies Office Multi-Year Research, Development and Demonstration Plan, 2012, http://www1.eere.energy.gov/hydrogenandfuelcells/mypp/pdfs/fuel_cells.pdf.
- 98 R. J. Stanis, M. A. Yaklin, C. J. Cornelius, T. Takatera, A. Umamoto, A. Ambrosini, C. H. Fujimoto, *J. Power Sources*, 2010, **195**, 104.
- 99 C. Fujimoto, D. -S. Kim, M. Hibbs, D. Wroblewski, Y. S. Kim, *J. Membr. Sci.*, 2012, **423-424**, 438.
- 100 Z. Hu, T. Ogou, M. Yoshino, O. Yamada, H. Kita, K. Okamoto, *J. Power Sources*, 2009, **194**, 674.
- 101 K. Chen, Z. Hu, N. Endo, J. Fang, M. Higa, K. Okamoto, *J. Membr. Sci.*, 2010, **351**, 214.
- 102 C. K. Lin, J. C. Tsai, *J. Mater. Chem.*, 2012, **22**, 9244.
- 103 J. Yan, X. Huang, H. D. Moore, C. Y. Wang, M. A. Hickner, *Int. J. Hydrogen Energy*, 2012, **37**, 6153.
- 104 Z. Hu, Y. Yin, K. Okamoto, Y. Moriyama, A. Morikawa, *J. Membr. Sci.*, 2009, **329**, 146.
- 105 Z. Jiang, X. Zhao, Y. Fu and A. Manthiram, *J. Mater. Chem.*, 2012, **22**, 24862.
- 106 R. Janarthanan, S. K. Pilli, J. L. Horan, D. A. Gamarra, M. R. Hibbs, and A. M. Herring, *J. Electrochem. Soc.*, 2014, **161**, F944.
- 107 G. K. S. Prakash, F. C. Krause, F. A. Viva, S. R. Narayanan, and G. A. Olah, *J. Power Sources*, 2011, **196**, 7967.
- 108 H. Kim, J. Zhou, M. Unlu, I. A. Richard, K. Joseph, and P. A. Kohl, *Electrochim. Acta*, 2011, **56**, 3085.
- 109 M. S. Kazacos, M. H. Chakrabarti, S. A. Hajimolana, F. S. Mjalli and M. Saleem, *J. Electrochem. Soc.*, 2011, **158**, R55.
- 110 P. Leung, X. Li, C. P. Leon, L. Berlouis, C. T. J. Lowa and F. C. Walsh, *RSC Adv.*, 2012, **2**, 10125.
- 111 B. Schwenzer, J. Zhang, S. Kim, L. Li, J. Liu, and Z. Yang, *ChemSusChem*, 2011, **4**, 1388.
- 112 X. Li, H. Zhang, Z. Mai, H. Zhang and I. Vankelecom, *Energy Environ. Sci.*, 2011, **4**, 1147.
- 113 J. Liu, J. G. Zhang, Z. Yang, J. P. Lemmon, C. Imhoff, G. L. Graff, L. Li, J. Hu, C. Wang, J. Xiao, G. Xia, *et al*, *Adv. Funct. Mater.*, 2012, **23**, 929.
- 114 W. Wang, Q. Luo, B. Li, X. Wei, L. Li, and Z. Yang, *Adv. Funct. Mater.*, 2012, **23**, 970.
- 115 C. Fujimoto, S. Kim, R. Stains, X. Wei, L. Li, Z. G. Yang, *Electrochem. Commun.*, 2012, **20**, 48.
- 116 C. N. Sun, Z. Tang, C. Belcher, T. A. Zawodzinski, C. Fujimoto, *Electrochem. Commun.*, 2014, **43**, 63.
- 117 H. Zhang, H. Zhang, X. Li, Z. Mai and J. Zhang, *Energy Environ. Sci.*, 2011, **4**, 1676.
- 118 H. Zhang, H. Zhang, F. Zhang, X. Li, Y. Li, and I. Vankelecom, *Energy Environ. Sci.*, 2013, **6**, 776.
- 119 Y. Li, X. Li, J. Cao, W. Xu, H. Zhang, *Chem. Commun.*, 2014, **50**, 4596.
- 120 H. Zhang, C. Ding, J. Cao, W. Xu, X. Li, H. Zhang, *J. Mater. Chem. A*, 2014, **2**, 9524.
- 121 B. Bae, K. Miyatake, M. Watanabe, *Polymer Science A: Comprehensive Reference, Alternative hydrocarbon membranes by step growth*, Elsevier, 2012, Chapter 10.34, pp.647.